ST. ANTHONY FALLS LABORATORY
Engineering, Environmental and Geophysical Fluid Dynamics

Project Report No. 546

Projecting the impact of climate change on coldwater stream temperatures in Minnesota using equilibrium temperature models

by

William Herb and Heinz Stefan

Prepared for

The Legislative-Citizens Commission on Minnesota Resources
St. Paul, Minnesota

September 2010
Minneapolis, Minnesota

Table of Contents

Executive Summary

Coldwater streams are valued because they provide unique habitat for coldwater fish such as trout, and other animal species. Water temperature is the most important characteristic of coldwater stream habitat. Stream temperature is controlled by the balance of the heat fluxes across the water surface and the heat fluxes across the sediment surface (groundwater inflow and conduction to the sediment). In this study, a modified equilibrium temperature model was developed for coldwater streams, including the effects of both climate and groundwater inflow on stream temperature. It gives an upper bound, and in some cases, good prediction of, daily average temperature based on climate conditions, riparian shading, stream width, and groundwater inputs.

The modified equilibrium temperature models developed in this study are intended to be applicable to stream-average (generic) analyses with minimal in-situ data on stream geometry, rather than for detailed analyses of individual stream reaches. Additional expressions are derived and tested for distances and times required to reach thermal equilibrium, and for diurnal temperature amplitude. For a small tributary stream with relatively uniform riparian shading (South Branch), the modified equilibrium temperature gave good predictions of daily average stream temperature. The modified equilibrium temperature model also gave good estimates of daily average stream temperature for the mainstem of the Vermillion when riparian shading was averaged over sufficiently long distances.

The stream temperature models were then used to characterize the response of water temperatures in three Minnesota coldwater stream basins to two projected climate change scenarios. Two of the study streams, Miller Creek and Chester Creek, are located in Duluth, Minnesota, and are primarily fed by upland wetlands. The third stream, the South Branch of the Vermillion River, is located south of the Twin Cities, Minnesota, and is primarily fed by shallow groundwater. Two climate change scenarios were run: the Canadian Global Climate Model (CGCM) version 2.0 for a doubling of atmospheric CO_2, and the Canadian Global Climate Model version 3.1 A1B scenario.

A sensitivity analysis conducted with the modified equilibrium temperature model confirms that water temperature in coldwater streams varies strongly with riparian shading, stream width, and both groundwater inflow rate and temperature. This sensitivity of stream temperature to groundwater parameters needs to be taken into account in climate change studies, since groundwater temperatures are expected to rise with air temperatures.

Overall, water temperatures in the streams were projected to increase between 4 and 5°C for the CGCM 2.0 CO_2 doubling climate change scenario, and between 3 and 4°C for the CGCM 3.1 A1B scenario. These stream temperature increases are larger than temperature increases projected by previous climate change studies based on air temperature – stream temperature regression analysis (2 to 3°C). Estimated increases in source water temperatures of groundwater due to climate change contributed about 60% of the total stream temperature increase, and the remaining 40% were provided by increases in atmospheric heat transfer. The ratio of the stream

temperature increment to air temperature increment was found to vary from 0.8 to 1.08, larger than the slope of the observed stream temperature versus air temperature relationship.

Increases in source water temperatures were therefore found to contribute significantly to the response of stream temperatures to climate change. For the streams in Duluth, wetland temperatures were predicted to increase 2.7 to 3.5 °C, based on a separate, calibrated heat transfer model. For the South Branch of the Vermillion River, groundwater temperatures were assumed to match long term increases in air temperature, ranging from 4 to 5 °C. These results suggest that source water temperatures need to be considered in predicting the response of stream temperature to climate change. More work is needed to characterize groundwater and other water sources for coldwater streams.

Notation

A	stream cross-section, m^2
B	stream width, m
C_p	specific heat of water, J/kg/°C
CR	cloud cover ratio, 0-1
C_{sh}	shading coefficient, 0-1
C_{ws}	wind sheltering coefficient, 0-1
d	water depth, m
e_a	ambient vapor pressure,
e_s	saturated vapor pressure,
h_{atm}	net atmospheric heat tranfer, W/m^2
h_{conv}	convective heat transfer, W/m^2
h_{evap}	evaporative heat transfer, W/m^2
h_{li}	incoming long wave radiation, W/m^2
h_{lo}	outgoing long wave radiation, W/m^2
h_s	solar heat transfer, W/m^2
h_{sed}	sediment heat transfer, W/m^2
K	bulk atmospheric heat transfer coefficient, W/m^2/°C
K_s	sediment thermal conductivity, W/m^2/°C
K_s*	combined sediment/groundwater heat transfer coefficient, W/m^2/°C
Q	stream discharge, m^3/s
q_g	groundwater inflow rate, m^2/s
R_s	incoming solar radiation, W/m^2
t	time, s
T	stream temperature, °C
T_a	air temperature, °C
T_d	dew point temperature, °C
T_e	equilibrium temperature, °C
T_e*	modified equilibrium temperature, °C
T_g	groundwater temperature, °C
T_{max}	daily maximum stream temperature, °C
V	flow velocity, m/s
W_p	wetted perimeter, m
x	streamwise distance, m
a	water surface albedo
δT	diurnal temperature change, °C
δ	depth of penetration, m
λ	characteristic length scale, m
τ	characteristic time scale, s
ρ	density, kg/m^3
ω	frequency, rad/s

Part I. Modified equilibrium temperature model for coldwater streams: Model formulation, verification, and sensitivity analysis

1.1 Introduction

Water temperature is a very important characteristic of aquatic habitats, particularly those supporting coldwater fish species such as trout [*Eaton et al.* 1995]. Stream temperature not only controls the survival of juvenile and adult coldwater fish, but also affects their reproduction and food sources such as macroinvertebrates [*Durance and Ormerod* 2007]. Hydrogeologic and climate settings constrain the existence of coldwater streams. In Minnesota, for example, trout streams are created by (1) karst springs in the southeast region of the state, near Rochester, 2) by cold wetlands in the northeast region of the state, near Duluth, and 3) by shallow groundwater aquifers in other regions of the state. The hydrological and climatological processes that maintain coldwater stream habitat vary between these regions, but involve a combination of cold water sources from groundwater or wetlands, riparian shading, and/or temperate climate. In other regions of the USA and the world, alpine settings with coldwater sources from snow or ice and cold mountain climate provide another important category of trout streams [*Brown and Hannah* 2007; *Clark et al.* 2001; *Hari et al*. 2006].

Both land development and climate change have the potential to increase stream temperatures and degrade coldwater habitat. Potential impacts on water temperatures have been estimated using field investigations and model studies [*Caissie* 2006; *Hari et al.* 2006; *Nelson and Palmer* 2007; *Webb et al.* 2008]. Deterministic, numerical stream temperature models can be used to predict the temperature response of specific streams to land use and climate change [*Herb and Stefan* 2008a, 2008b; *Kim and Chapra* 1997; *Sinokrot and Stefan* 1994]. Analytical models have been applied with some success for steady state and transient stream temperature prediction [Edinger et al. 1974; *Tang and Keen* 2009]. Regional regression models have also been created to study the impacts of land use and climate change on stream temperature [*Mohseni et al.* 1999; *Wang et al.* 2003]. Stream temperature – air temperature regression models can be used to characterize stream temperature in current conditions [e.g. *Webb et al.* 2003] and make estimates of the sensitivity of stream temperature to future increases in air temperature predicted by global climate models [*Erickson and Stefan* 2000; *Mohseni and Stefan* 1998, 1999]. These relationships can be improved by considering equilibrium temperature, which takes into account atmospheric moisture, wind and radiation in addition to air temperature [*Bogan et al.* 2003; *Edinger et al.* 1968]. However, even equilibrium temperature is often not a sufficient predictor of stream temperature because urban storm- and wastewater, as well as groundwater and tributary inputs can contribute significantly to a streams heat budget [*Bogan et al.* 2004].

Limited information is currently available to characterize the general response of stream temperature to a combination of surface (atmospheric) and subsurface (groundwater) heat inputs, which is particularly important for coldwater streams which typically drain small watersheds. The aim of this study was to evaluate relatively simple, process-based stream temperature models based on the equilibrium temperature concept which include riparian shading and groundwater inputs. Previously developed relationships for equilibrium temperature were augmented by additional terms to take into account groundwater inputs and heat conduction to the sediment. A trout stream in Minnesota was used to evaluate the ability of these models to predict daily average stream temperature. A sensitivity analysis was used to characterize the relative importance of climate parameters, groundwater inputs, and stream channel characteristics for determining stream temperatures.

1.2. Model Formulation

1.2.1 Heat balance for a stream reach

A one-dimensional equation for stream temperature at some cross-section of a stream can be written as

$$\frac{\partial}{\partial t}(AT)+\frac{\partial}{\partial x}(QT)=\frac{B\,h_{atm}(T)}{\rho C_p}+q_g T_g+\frac{W_p\,h_{sed}(T)}{\rho C_p} \qquad (1)$$

where A = flow cross-sectional area, B = stream width, h_{atm}= atmospheric heat transfer rate, h_{sed}= sediment heat transfer rate (W/m^2), q_g = groundwater inflow rate (m^2/s), Q = stream discharge, t = time, T_g= groundwater temperature, T = stream temperature, W_p= wetted perimeter, x= streamwise distance and $\rho\, C_p$= product of density and specific heat for water. A longitudinal dispersion term is not necessary in this equation because the longitudinal temperature gradients are usually small (zero in the case of equilibrium temperature). For the purposes of this study, lateral inflows are assumed to be entirely due to groundwater inputs. If surface inflows are present,, they can be accommodated by a modified inflow temperature. For steady flow conditions, $\partial A/\partial t = 0$. The second term on the LHS of Equation 1 can be expressed as $Q\cdot\partial T/\partial x$ + $T\cdot q_g$. The first term on the RHS of Equation 1 is the heat flux across the water surface of the stream, and the second term on the RHS is the groundwater heat input to the stream. The third term on the RHS is the heat transfer between the streambed and the flowing water, which can be estimated by a heat conduction equation, $h_{sed} = (K_s/\delta)\cdot(T_g-T)$, where K_s is the effective thermal conductivity of the sediment, δ is a characteristic length scale for the conduction process, and the sediment temperature has been assumed equal to the groundwater inflow temperature. Using these assumptions, Equation 1 can be simplified to the form:

$$A\frac{\partial T}{\partial t}+Q\frac{\partial T}{\partial x}=\frac{B\,h_{atm}}{\rho C_p}+\left(q_g+\frac{W_p K_s}{\rho C_p \delta}\right)\left(T_g-T\right) \qquad (2)$$

A key to determining stream temperatures are appropriate formulations for the atmospheric heat transfer as a function of climate parameters. The net heat transfer rate at the water surface (h_{atm}(T)) is the sum of components due to solar radiation (h_s), incoming longwave radiation (h_{li}), back radiation (h_{lo}), evaporation (h_{evap}), and convection (h_{conv}):

$$h_{atm}=h_s+h_{li}-h_{lo}-h_{evap}-h_{conv} \qquad (3)$$

The heat transfer formulations used in this study are based on those given by *Edinger et al.* [1968 and 1974] for lake and reservoir surfaces.

$$h_{evap}=C_o\,f(W)\beta\left(T-T_d\right) \qquad (4)$$

$$h_{conv}=C_o\,f(W)\left(T-T_a\right) \qquad (5)$$

$$\beta = \frac{e_s - e_a}{T - T_a} \quad (\text{mmH}_g/°\text{C}) \tag{6}$$

$$f(W) = a_o + a_1 W \quad (\text{W/m}^2/\text{mmH}_g) \tag{7}$$

$$h_s = (1-\alpha)(1-C_{sh})R_s \tag{8}$$

$$h_{li} = \sigma\left(CR + 0.67 \cdot (1-CR)e_a^{\ 0.08}\right)\left(T_a + 273.15\right)^4 \tag{9}$$

$$h_{lo} = \varepsilon\sigma\left(T + 273.15\right)^4 \tag{10}$$

where C_o is Bowen's ratio (0.47 mm Hg/°C) α is the water surface albedo, R_s is incident solar radiation, C_{sh} is the shading coefficient (1=full shading), σ is the Stefan-Boltzmann constant, ε is the emissivity, *CR* is the cloud cover fraction (0-1), and e_s and e_a (mm Hg) are the saturated vapor pressure at *T* and the atmospheric vapor pressure, respectively. Equation 7 gives the form of the wind speed function used in this study. In general, the wind speed function *f(W)* can include constant, linear, and quadratic wind speed coefficients (*Edinger et al.,* 1974), and/or account for atmospheric stability which becomes important for artificially heated water bodies (Ryan and Harleman, 1973; Stefan et al.,1980). The observed wind velocity (W_o) was adjusted based on a wind sheltering coefficient, C_{ws}, i.e. $W = (1-C_{ws})\cdot W_o$.

1.2.2 Equilibrium temperature

The equilibrium temperature (T_e) of a surface water body is defined as the water temperature at which the water body reaches thermal equilibrium with the atmosphere, e.g. zero net heat flux across the water surface. Equilibrium temperature can be used to predict analytically or numerically the temperature of surface water bodies, e.g. lakes and streams [*Edinger et al.* 1968, 1974]. In general, actual water temperatures approach equilibrium temperature asymptotically, and the lag time is inversely proportional to water depth; therefore the assumption that water temperature equals equilibrium temperature cannot be used to describe short term thermal behavior, e.g. diurnal fluctuations in stream temperature, but it is appropriate for daily time scales and longer. The SNTEMP stream temperature model [*Theurer et al.* 1984] uses equilibrium temperature as a basis for predicting daily average stream temperature using similar formulations to those given here.

By definition, the equilibrium temperature is the stream temperature which causes the surface heat transfer term (h_{atm}) in Equation 2 to be zero. One approach to determine equilibrium temperature is to calculate the components of surface heat transfer (radiation, convection, evaporation) as a function of climate parameters (air temperature, humidity, solar radiation, wind speed, cloud cover) and then find the water temperature at which the sum or net surface heat transfer is zero. This process requires an iterative solution, since some heat transfer terms are a non-linear function of water temperature, e.g. Equation 10. *Edinger et al.* [1974] give several simplified formulations to estimate equilibrium temperature and introduce a bulk coefficient for surface heat transfer, *K*. In that process the back radiation term is expressed as

$$h_{lo} \approx 306 + 4.48T + 0.025T^2 \tag{11}$$

A relatively accurate estimate of equilibrium temperature (T_e) is

$$T_e = \frac{\left(h_s + h_{li} - 306 + (K - 4.48)T_d^{'}\right)}{K + 0.05T_d^{*} - 0.025\,T_e} \qquad (12)$$

$$K = 4.5 + 0.05T + \left(0.47 + \beta\right) f(W) \qquad (\mathrm{W/m^2/°C}) \qquad (13)$$

$$T_d^{'} = T_d + \frac{0.47\left(T_a - T_d\right)}{\beta + 0.47} \qquad (14)$$

Since T_e appears on the RHS of Equation 12, an iterative solution can be used to improve accuracy. When T_a was used as the initial guess for T_e in this study, only a few iterations were required to converge to a solution.

1.2.3 Modified equilibrium temperature - shift due to groundwater inflow and streambed heating

Equilibrium temperature, in the original sense, considers only atmospheric heat inputs. The effect of a groundwater input (per unit stream length) on stream temperature can be analyzed by introducing the modified equilibrium temperature concept. Heat transfer by conduction from the stream to the streambed can also be included with the assumption that the sediment temperature is equal to a groundwater temperature:

$$h_{sed} = \frac{K_s}{\delta}\left(T - T_g\right) \qquad (15)$$

where K_s is the effective thermal conductivity of the sediment bed, and δ is the characteristic length scale for conduction. A modified equilibrium temperature, T_e*, is found by setting the entire RHS of Equation 2 equal to zero. The * notation distinguishes this groundwater adjusted temperature from the standard equilibrium temperature based on atmospheric heat transfer only (T_e).

$$h_{atm}\left(Te*\right) + \left(\rho C_p \frac{q_g}{B} + \frac{W_p K_s}{B\delta}\right)\left(T_g - T_e*\right) = 0 \qquad (16)$$

Since B is the stream width, the term (q_g/B) is the groundwater inflow rate per unit area of stream bed. The temperature T_e* found by solving Equation 16 represents a modified equilibrium temperature for which the atmospheric heat transfer balances the heat input due to groundwater inflow and conduction into the streambed. A stream receiving groundwater will tend toward that modified equilibrium temperature given sufficient time (and spatial distance). In mid-summer, atmospheric heat flux would typically be into the stream tending to heat the water, while the incoming groundwater would tend to cool the stream ($T_g < T$). In winter, the groundwater would heat the stream, and the heat flux to the atmosphere would cool it.

Equation 16 can be solved for the modified equilibrium temperature T_e*. Using methods from *Edinger et al.* [1974], Equations 17, equivalent to Equation 12 can be found for the modified equilibrium temperature.

$$T_e^* = \frac{\left(h_s + h_{li} - 306 + (K - 4.48)T_d^{'}\right) + K_s^* T_g}{K + K_s^* + 0.05T_d^* - 0.025T_e^*} \tag{17}$$

$$K_s^* = \frac{K_{sed}}{\delta} + \frac{W_p}{B}\frac{\rho C_p q_g}{B} \tag{18}$$

In many shallow streams, the wetted perimeter W_p can be approximated by stream width *B*. The parameter K_s* is a combined heat transfer coefficient for the groundwater and sediment. For q_g= 0.01 m^3/s/km (0.17 cfs/mile), K_s = 1 W/m/°C, δ=1 m, and a stream width of 5 m, K_s* ≈ 14 (W/m^2/°C), which is of the same order of magnitude as the bulk atmospheric heat transfer coefficient, *K*. Additional examples of the magnitude of *K* and K_s* are given in Table 1.2 for two reaches of the Vermillion River.

Although the modified equilibrium temperature is intended to be applied to relatively uniform stream reaches, the assumed uniform groundwater inflow rate introduces a systematic increase of flow rate with downstream distance. As the stream width *B* also increases with increasing flow downstream, the relative effect of groundwater inputs on stream temperature is reduced with distance. For a fixed rate of groundwater inflow per unit length (q_g), an increase in stream flow and width leads to a slight positive streamwise temperature gradient. For the South Branch reach of the Vermillion River described later, the streamwise gradient in temperature is small, about 0.02 °C/km in mid-summer. On the other hand, if the groundwater inflow rate per unit surface area (q_g/B) is held constant, T_e* is invariant over streamwise distance (assuming shading, etc. are also constant).

1.2.4 Length and time scales required to reach equilibrium temperature

Stream temperature responds to changes in heat inputs over length and time scales which can be estimated using relatively simple relationships. If a slug of water is followed downstream along a characteristic path, it can be shown that Equation 2 can be simplified to the following form [*Theurer et al.* 1984]:

$$\frac{\partial T}{\partial x} = \frac{B\,h_{atm}}{\rho C_p Q} + \left(\frac{q_g}{Q} + \frac{W_p\,K_s}{\rho C_p Q \delta}\right)(T_g - T) \tag{19}$$

Equation 19 can be rewritten in terms of the parameters used in the equilibrium temperature formulations as

$$\frac{\partial T}{\partial x} = \frac{K\,\mathrm{B}}{\rho C_p Q}\left(T_e - T\right) + \frac{K_s^* B}{\rho C_p Q}(T_g - T) \tag{20}$$

Equation 20 can be solved for *T*(*x*), the longitudinal variation in the mean stream temperature, with the result given by Equation (21).

$$T(x) = T_e^* + \left(T_o - T_e^*\right)\exp\left(-\frac{x}{\lambda}\right) \tag{21}$$

$$T_e^* = \frac{K\,T_e + K_s^*\,T_g}{K + K_s^*} \tag{22}$$

$$\lambda = \frac{\rho C_p Q}{B\left(K + K_s^*\right)} \tag{23}$$

where T_o is the upstream temperature (at $x=0$) and λ is the length scale for the response of stream temperature to a step change in temperature or heat flux at $x=0$. The corresponding characteristic time scale or time constant (τ) can be found by dividing the length scale by flow velocity $V=Q/A$.

$$\tau = \frac{\lambda}{V} = \frac{\rho C_p d}{K + K_s^*} \tag{24}$$

While the equilibrium temperature (T_e *or* T_e*) does not explicitly depend on the streamflow (Q), it is noteworthy that the thermal length scale λ has a linear dependence on (Q/B). A stream with higher flow, and in particular, greater depth, therefore requires a greater distance to respond to a water temperature disturbance. Equations 23 and 24 can be applied to a variety of perturbations on stream temperature, including changes in riparian shading, changes in the groundwater inflow rate, and concentrated surface inflows.

For the mainstem reach of the Vermillion River, described in a later section, λ is found to vary from 3 to 45 km, and τ from 7 to 50 hours, for stream flows from to 0.43 to 5.8 m^3/s (15 to 205 cfs) during the summer period. Streams are more likely to approach equilibrium conditions during periods of low flow. The length scale parameter, λ, can be used to determine the distance upstream of a monitoring point that will have influence on the temperature at that point. For example, the length scale can be used to determine over what upstream distance riparian shading needs to be averaged to estimate stream temperature at a point.

1.2.5 Diurnal stream temperature fluctuation and daily maximum stream temperature

Diurnal temperature fluctuations can be a determining factor for the quality of aquatic habitat in a stream reach. Some stream temperature studies, such as TMDL (Total Maximum Daily Load) studies, use maximum, rather than average, daily stream temperature as a basis for quantifying temperature impacts. It is possible to find estimates for both the amplitudes of diurnal temperature variations and the maximum daily stream temperature, using an approach similar to the foregoing analysis of equilibrium temperature.

Diurnal stream temperature variations are driven by atmospheric heat transfer across the water surface. Figure 1.1 gives an illustration of the calculated diurnal fluctuations of solar radiation, incoming log wave radiation, evaporation, and convection for a stream reach with 50% shading, using the previously given heat transfer Equations 4 to 11. The convection and evaporation terms were calculated based on the equilibrium temperature, rather than the actual, stream temperature to give a better representation of the magnitude of these heat transfer components. The example in Figure 1.1 is for a two-week period in July. Over the time period June 1 to October 1, 2008, the diurnal fluctuations averaged 307, 66, 59, and 47 W/m^2 for solar radiation, incoming long wave radiation, evaporation, and convection, respectively. Incoming long wave radiation and convection have a correlation to solar radiation (correlation coefficients = 0.35, 0.70, respectively), while evaporation is poorly correlated to solar radiation (correlation coefficient = 0.08). For this reason, diurnal fluctuations of stream temperature driven by evaporation are not considered.

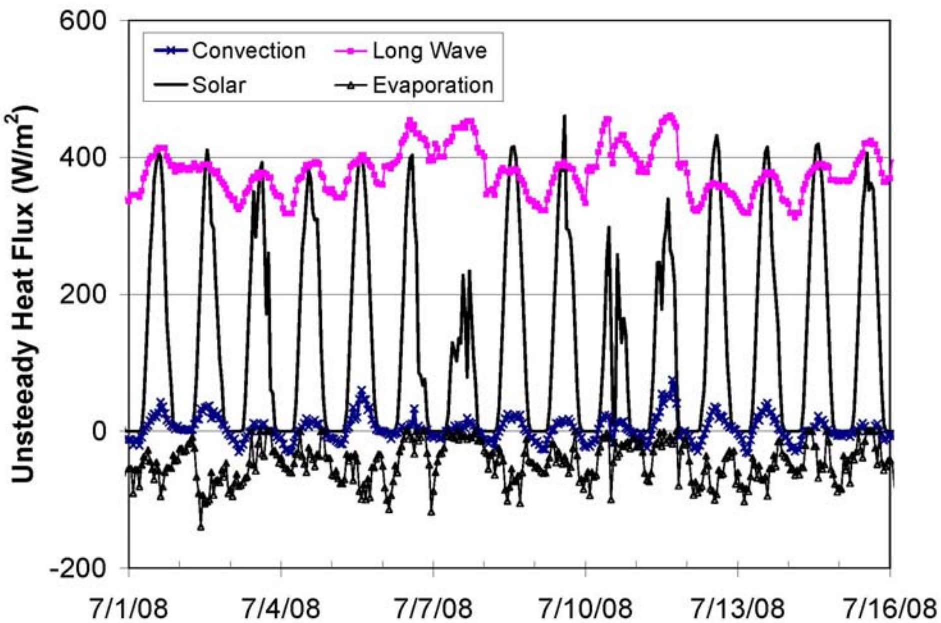

Figure 1.1. Example of time series of solar radiation, incoming long wave radiation, convection, and evaporation for a water body at equilibrium temperature in Minneapolis, 45°N latitude, 93°W longitude).

To find analytic expressions for the diurnal temperature variations of a stream, sinusoidal variations of stream temperature, solar radiation, and air temperature are assumed:

$$T(t) = \overline{T} + \hat{T}\exp(j\omega t) \tag{25}$$

$$h_s(t) = \overline{h}_s(1 + \exp(j\omega t)) \tag{26}$$

$$T_a = \overline{T}_a + \hat{T}_a\exp(j\omega t) \tag{27}$$

where $\overline{T}$, $\overline{T}_a$ and $\overline{h}_s$ are the daily mean values of stream temperature, air temperature and solar heat flux, $\hat{T}$ and $\hat{T}_a$ are the amplitude of stream temperature and air temperature, respectively, ω is the frequency of oscillation (7.27x10^{-5} rad/s for a period of 1 day), and $j = \sqrt{-1}$. Note that it is not necessary to specify a fluctuating component of the solar heat flux, because for a simple sinusoid, $\hat{h}_s$ must be equal to $\overline{h}_s$ for the function to oscillate between zero and the maximum value. Complex number notation is used to simplify solution procedures; the actual temperature fluctuations are represented by the real part of the solution. Substituting Equations 25 - 27 into Equation 2 and solving for the fluctuating components only, gives the following expression for fluctuating stream temperature:

$$\hat{T} = \left(\frac{\overline{h}_s + \left(0.47 f(W) + 4.6\varepsilon_a\right)\hat{T}_a}{\rho C_p d \; j\omega + K_s^* + 0.47 \, f\left(W\right) + 4.48} \right) \tag{28}$$

where d is the mean water depth. $\hat{T}$ is a complex number that represents both the magnitude of the stream temperature oscillation and the phase with respect to the solar gradation driver. For the purposes of this study, it is sufficient to predict the total diurnal change in temperature ($\delta T = T_{max} - T_{min}$), which can be found as:

$$\delta T = 2\left|\hat{T}\right| = \frac{2\left(\overline{h}_s + \left(0.47 f(W) + 4.6\varepsilon_a\right)\hat{T}_a\right)}{\left[\left(\rho C_p d \;\; \omega\right)^2 + \left(K_s^* + 0.47 \, f\left(W\right) + 4.48\right)^2\right]^{1/2}} \tag{29}$$

If the convection, long wave radiation, and groundwater terms are dropped, Equation 29 simplifies substantially to an expression that considers only solar radiation as the driver:

$$\delta T = \frac{2\,\overline{h}_s}{\rho C_p d \;\; \omega} \tag{30}$$

1.3 Model Validation

The analytic expressions for equilibrium stream temperature and diurnal temperature fluctuations provide estimates of stream temperature in uniform stream reaches. Real stream reaches have natural variations of stream characteristics with downstream distance, inflows from tributaries, and are impacted by land use and development which can cause abrupt changes in channel width, stream depth, riparian shading etc. The expressions for the longitudinal variation of stream temperature in non-equilibrium conditions provide some opportunity to correct for non-uniform stream characteristics in terms of geometry, shading, and groundwater inflow, but they require additional information, e.g. the upstream temperature. To test the impact of these discrepancies, the temperatures predicted by the analytic (simplified) models will be compared to observed stream temperature data, and to simulation results from a detailed numerical stream temperature model.

1.3.1 Stream reaches and data for model validation

The comparison of analytic and numerical temperature model results was made for two reaches of the Vermillion River, a tributary of the Mississippi, and a designated trout stream about 20 miles south of the Twin Cities (Minneapolis and St. Paul) in Minnesota (Figure 1.2). The upper Vermillion River has numerous groundwater-fed coldwater reaches. Substantial temperature and flow monitoring has occurred on the Vermillion over several years, and numerical models for stream flow and temperature have been developed [*Herb et al.* 2008a, b]. For the present study, a 4.3 km reach of the South Branch, a tributary to the Vermillion, and a 8 km reach of the Vermillion mainstem upstream of the USGS (United States Geological Survey) flow monitoring station at Empire, MN were selected (Figure 1.2). Water temperature has been monitored in these reaches in 2006, 2007, and 2008. The 2008 data will be used in this study, because 1) additional parameters related to groundwater inputs have been measured in 2008, and 2) the confounding effect of a wastewater input from the Empire wastewater treatment plant is no longer present in 2008 because of a permanent wastewater diversion.

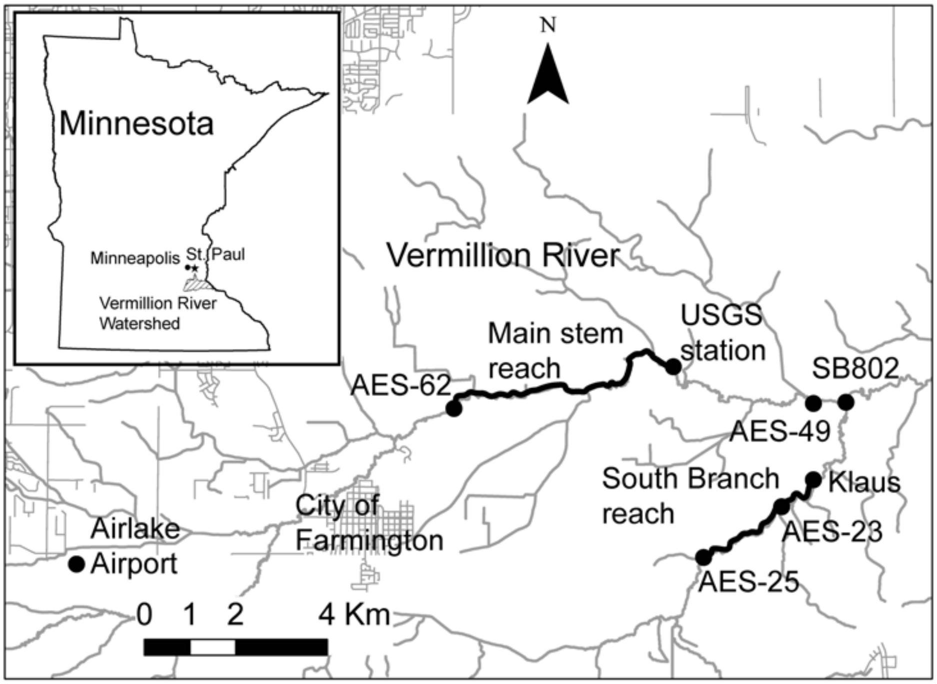

Figure 1.2. Map of the test reaches and temperature monitoring stations in the South Branch and in the mainstem of the Vermillion River. The Vermillion River is a tributary of the Mississippi, and is located about 30 km south of the Twin Cities (Minneapolis and St. Paul) in Minnesota.

Continuous 15 minute stream flow data for 2008 were obtained for the USGS gaging site on the Vermillion River main stem at Empire and for the SB802 site on the South Branch of the Vermillion River (Figure 1.2). Stream temperature recorded at 15-minute intervals were obtained for the USGS site and for a site 8 km upstream at Biscayne Ave (AES-62 site in Figure 1.2). Stream temperature data were also obtained for three sites on the South Branch (SB802, AES-23, AES-25, Figure 1.2). Stream temperatures were monitored by the Dakota County Soil and Water Conservation District and the Minnesota Department of Natural Resources using Onset Hobo temperature loggers. Streambed temperature was also monitored at other sites in the Vermillion River watershed, including a site approximately 6 km downstream of the USGS site (AES-49) and a site on the South Branch (AES-23), shown in Figure 1.2. Streambed temperatures were monitored at a depth of about 40 cm into the sediment bed using piezometers equipped with Onset Hobo temperature loggers. This monitoring work was performed by Applied Ecological Services, Inc. in St. Paul, MN. Both monitored reaches are “gaining reaches”, i.e. they have significant groundwater inflow [*Janke et al. 2008*]; streambed temperatures give a good estimate of the groundwater inflow temperature. Climate data were available from the Airlake Airport near Lakeville, including air temperature, relative humidity, and wind speed at 1-hour intervals. 10-minute solar radiation data were recorded at the St. Anthony Falls Laboratory, University of Minnesota, in Minneapolis, approximately 30 km north of the Vermillion River.

1.3.2 Comparisons with numerical 1-D model simulation results

A numerical stream temperature model for the Vermillion River basin was previously developed at the University of Minnesota to study the impact of land use changes on stream temperature [*Herb et al.* 2008a, b]. The stream temperature model is 1-D and unsteady; it includes surface heat transfer, sediment heat transfer, uniform or spatially varying groundwater inputs, surface runoff inputs, and riparian shading. The spatial resolution of the model is 100 m and the time resolution is 5 to 60 minutes, depending on the size of the reach. For the stream reaches of the present study, a 1-hour time step was found to be adequate for the numerical simulations. Unsteady stream flow and cross-sectional areas are supplied as an external model input. The EPD-riv1 model [*US EPA* 2005] was used to generate hourly stream flows in the mainstem and in reaches of the South Branch based on the observed flow at the USGS and SB802 flow gaging sites, respectively.

<u>Stream reach in the South Branch of the Vermillion River</u>

The South Branch reach was selected as a test case for model validation because stream temperatures recorded at three sequential stations (AES-25, AES-23, Klaus in Figure 1.2) were nearly identical (root-mean-square difference of 1.0^{o}C), indicating that the analytic models for equilibrium temperature and diurnal temperature variation should be applicable to this reach. The numerical stream temperature model was calibrated for the South Branch reach for the period June 1 to September 30, 2008 using the observed stream temperature at (AES-25) as the upstream boundary condition. The groundwater inflow rate (q_g) was set to 12 L/s per km (0.68 cfs/mile). The actual groundwater inflow rate from a shallow sand aquifer would be expected to vary at weekly to monthly time scales, but adequate results for the study period were obtained using a constant input rate. Monthly precipitation and stream discharge during the period June 1 to September 30, 2008 was relatively uniform, except for higher flow in June (Figure 1.3). The shading coefficient (C_{sh}) was assumed to be equal to the wind sheltering coefficient (C_{ws}) and was calibrated to be 0.63. The numerical stream temperature model gave a good fit of the observed downstream temperature at the Klaus station (Figure 1.4). The overall RMSE of the simulated 1-hour temperatures was 0.8°C over the 4 month period.

<u>Stream reach in the Vermillion River mainstem</u>

A stream temperature model was also developed and calibrated for the mainstem reach of the Vermillion River. The observed hourly stream temperatures at the AES-62 site (Biscayne Ave.) were used as the upstream boundary condition and the riparian shading coefficient and the groundwater inflow rate were adjusted to best match the observed downstream temperature at the USGS station. The streambed temperature observed at station AES-49, 6 km downstream of the USGS station, was used as the groundwater temperature; it varied seasonally from 9 °C in June to 11.5 °C in September. The shading coefficient (C_{sh}) was calibrated to a value of 0.35, and set equal to the sheltering coefficient. The calibrated groundwater inflow rate (q_g) for the Vermillion River main stem reach was 13.2 L/s per km (0.75 cfs/mile). The stream temperature simulation results are compared to observed stream temperatures at the USGS station in Figure

1.5. Good accuracy was achieved for both daily mean temperatures and diurnal temperature fluctuations, with root-mean square errors (RMSEs) of about 1°C.

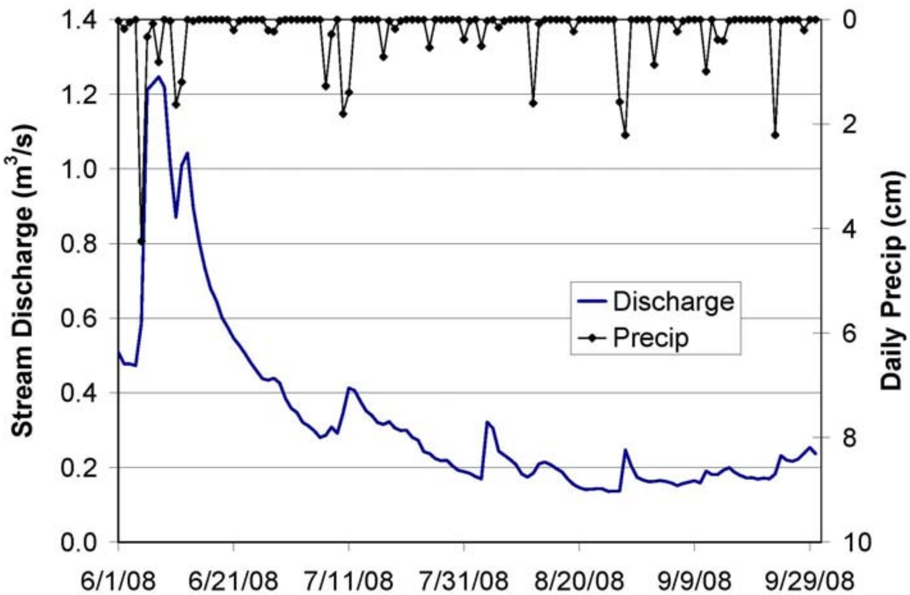

Figure 1.3. Daily stream discharge and precipitation for the South Branch of the Vermillion River, 2008.

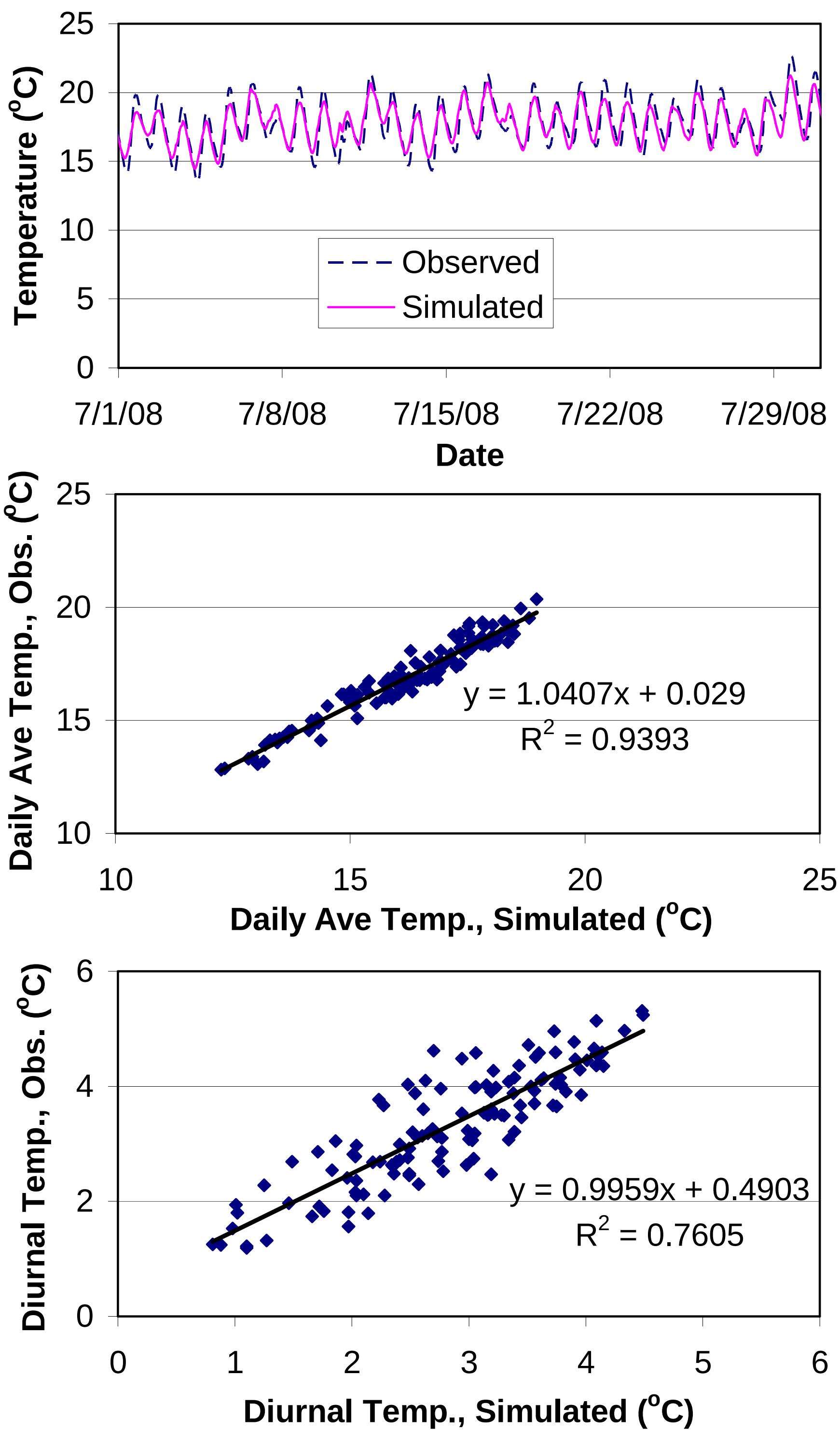

Figure 1.4. Time series of numerically simulated and observed hourly stream temperatures in the South Branch reach (upper panel), observed vs. simulated daily average stream temperature (center panel), and observed vs. simulated diurnal temperature variation (δT, lower panel). The overall RMSE of the 1-hour temperature simulation is 0.8°C.

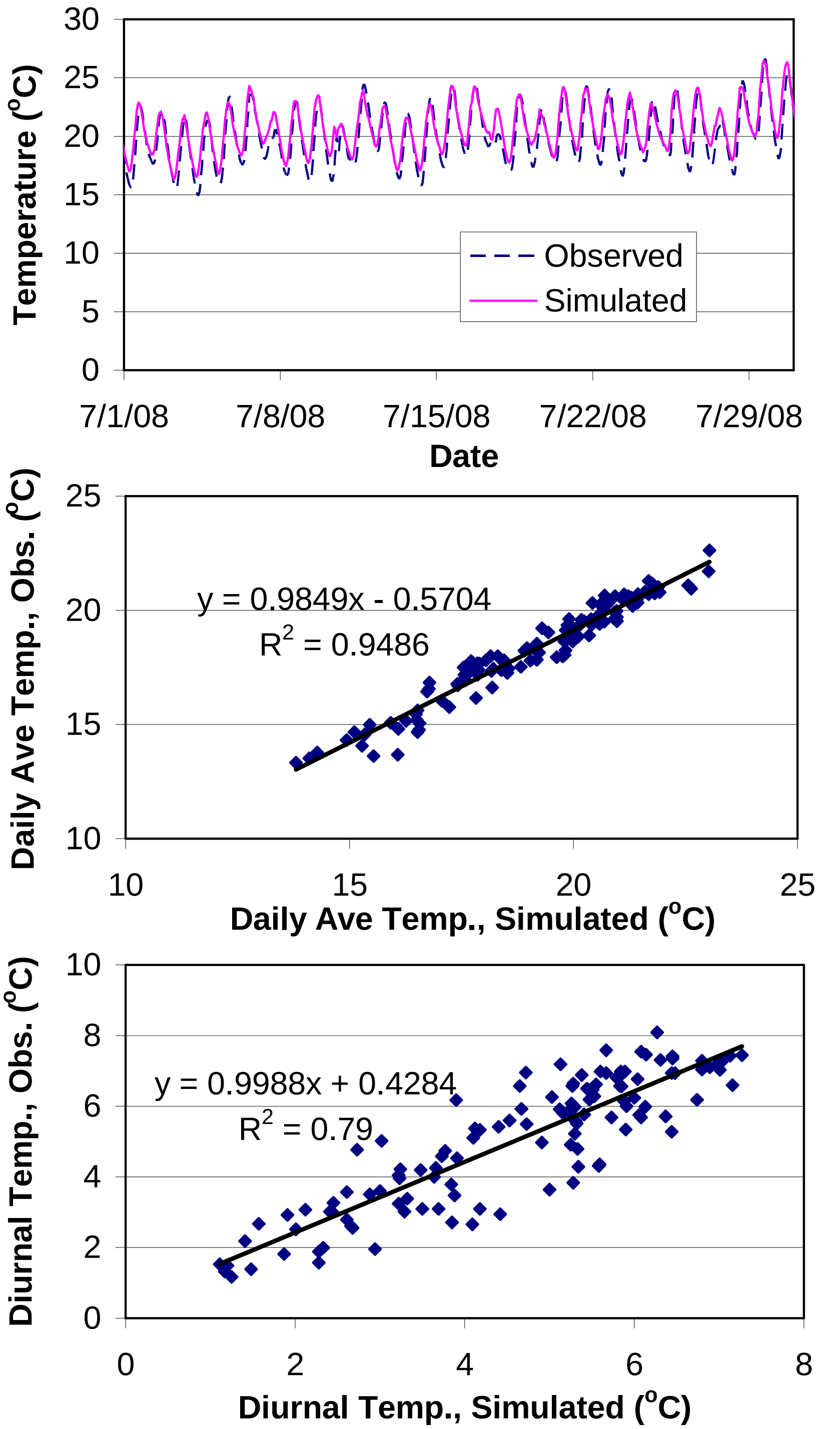

Figure 1.5. Time series of numerically simulated and observed hourly stream temperatures in the mainstem reach (upper panel), observed vs. simulated daily average temperature (center panel), and observed vs. simulated diurnal temperature variation (δT, lower panel). The overall RMSE of the 1-hour temperature simulation is 1.2 °C.

1.3.3 Modified equilibrium temperature model results

The analytic, modified equilibrium temperature model (Equations 17 and 18) was used to predict daily average stream temperatures in the South Branch and mainstem reaches of the Vermillion River for the period June 1 to September 30, 2008. The groundwater input rates and temperatures, and the riparian shading and wind sheltering coefficients were set equal to the calibrated values from the numerical model study. The stream width was set for each day based on the observed discharge using power law relationships.

Statistics of the predicted and observed mean daily temperatures are summarized in Table 1.1. For the South Branch of the Vermillion River, modified equilibrium temperature was a good predictor of daily stream temperature with an RMSE of 1.2°C. For the mainstem reach, equilibrium temperature was also a reasonable of mean daily stream temperature; the RMSE was 1.4 °C.

The average values of the atmospheric bulk heat transfer coefficient (K) and the sediment/groundwater coefficient (K_s*) are given in Table 1.2. For the wider mainstem reach, the average value of K (13.1 W m^{-2} $^{o}C^{-1}$) is 2.5 times higher than K_s* (5.8 W m^{-2} $^{o}C^{-1}$); for the South Branch reach, K (9.0 W m^{-2} $^{o}C^{-1}$) is 1.7 times lower than K_s* (15.2 W m^{-2} $^{o}C^{-1}$).

The analytic diurnal equilibrium temperature model (Equation 29) was used to predict diurnal stream temperature fluctuations in the two Vermillion River reaches for the period June1 to September 30, 2008. For both the mainstem and South Branch reaches, Equation 29 was a good predictor of diurnal stream temperature changes. Statistics of the predicted and observed mean diurnal temperature fluctuations are summarized in Table 1.3. The analytic model results compared to observations had a slightly higher RMSE than the numerical model results.

<u>Stream reach in the South Branch of the Vermillion River.</u>

The mean flow rate for South Branch was 0.34 m^3/s (12 cfs) for the period June 1 to September 30, 2008. For SB802 on the South Branch of the Vermillion River, the daily equilibrium temperature computed from Equation 17 was a good predictor of the observed daily average stream temperature (Figure 1.6). The RMSE was 1.2°C. Statistics of the predicted and observed mean daily temperatures are given in Table 1.1.

<u>Stream reach in the Vermillion River mainstem</u>

The mainstem of the Vermillion River at the USGS gaging station site is substantially larger than South Branch, with a mean flow of 0.34 m^3/s (12 cfs). Three cases were run for the mainstem segment, which demonstrate the abilities and limitations of the modified equilibrium temperature model:

1. Modified equilibrium temperature, local shading conditions. For the reach between Biscayne Ave (AES-62) and the USGS station, the calibrated shading coefficient from the numerical model was 0.35. Using this shading coefficient, the equilibrium temperature model systematically over-predicted daily average stream temperatures (Figure 1.7, lower panel), with RMSE = 3.1°C. The main reason for this overprediction is that this stream reach is not in thermal

equilibrium. Stream temperature in that reach increases systematically with distance (*dT/dx* > 0), due to low riparian shading (C_{sh} = 0.35) relative to upstream reaches (C_{sh} = 0.5 to 0.8). According to Equation 23, the characteristic length (λ) required to reach equilibrium in that stream reach is about 12 km at low flow (0.5 m^3/s) and 100 km at high flow (6 m^3/s).

2. Modified equilibrium temperature with spatially averaged shading conditions.
Riparian shading conditions were spatially averaged over 20 km upstream of the USGS site, based on calibrated shading from previous numerical model results (Herb et al. 2008a), yielding a mean shading of 0.70. If this mean value is then used in the modified equilibrium temperature model (eq. 17), predicted temperatures match observations at the USGS site reasonably well (RMSE =1.4 C, Figure 1.7 center panel).

3. Modified equilibrium temperature with spatial correction, local shading conditions. If Equations 21 and 22 are used to adjust the modified equilibrium temperatures based on the observed stream temperature at Biscayne Ave, the calculated modified equilibrium temperatures match measured stream temperatures quite well (Figure 1.7, upper panel). The longitudinal variation of stream temperature predicted by the analytic model (Equations 21 to 23) also agrees well with those simulated by the numerical model (Figure 1.8).

The analytic diurnal temperature fluctuation model (Equation 29) was a good predictor of diurnal stream temperature changes (Figure 1.9); the RMSE was 0.86°C for the South Branch reach, and 1.0°C for the mainstem reach, respectively. For both the SB802 and USGS stations, the analytic model for diurnal temperature fluctuations had a slightly (order 0.1°C) higher RMSE to observations than the numerical model (Table 1.3). The RMSE values for the numerical model were 0.94°C and 0.68°C for the mainstem reach and the South Branch reach, respectively.

Table 1.1. Summary statistics of mean daily stream temperatures (°C) in the mainstem and South Branch reaches of the Vermillion River, June 1 - September 30, 2008.

Parameter	Mainstem	South Branch
Average, Observed	18.2	16.9
St. Dev., Observed	2.1	1.7
Average, Numerical	19.1	16.3
St. Dev., Numerical	2.1	1.6
RMSE, Numerical	1.3	0.8
Average, Analytic	18.5	15.6
St. Dev., Analytic	2.4	1.5
RMSE, Analytic	1.4	1.2

Table 1.2. Magnitude and variability of the atmospheric heat transfer coefficient (*K*) and the sediment/groundwater bulk heat transfer coefficient (K_s*) for the mainstem and South Branch reaches of the Vermillion River for June 1 – September 30, 2008. In all cases, K_s = 1 W/m/°C and δ=2 m.

Parameter	Mainstem	South Branch
q_{gw} (L/s/km)	13.2	12.7
B (average, m)	3.8	11.2
K_s* (average, W/m^2/ºC)	5.8	15.2
K_s* (stan dev,W/m^2/ºC)	0.25	1.5
K (average, W/m^2/ºC)	13.1	9.0
K (stan dev, W/m^2/ºC)	4.2	2.4

Table 1.3. Summary statistics of diurnal stream temperature fluctuations (°C) in the mainstem and South Branch reaches of the Vermillion River, June 1 - September 30, 2008.

Parameter	Mainstem	South Branch
Average, Observed	5.0	3.3
St. Dev., Observed	1.8	0.99
Average, Numerical	4.6	2.8
St. Dev., Numerical	1.6	0.87
RMSE, Numerical	0.94	0.68
Average, Analytic	4.2	2.8
St. Dev., Analytic	1.6	1.0
RMSE, Analytic	1.0	0.86

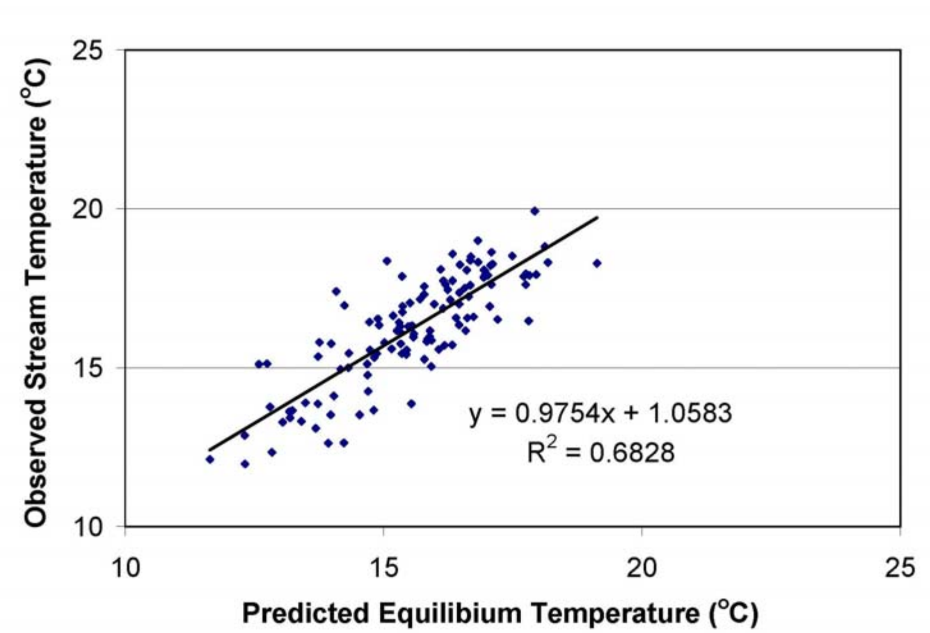

Figure 1.6. Observed daily average stream temperature vs. modified equilibrium temperature from Eq. 17 for the SB802 site, June 1 – September 30, 2008. RMSE =1.2 °C.

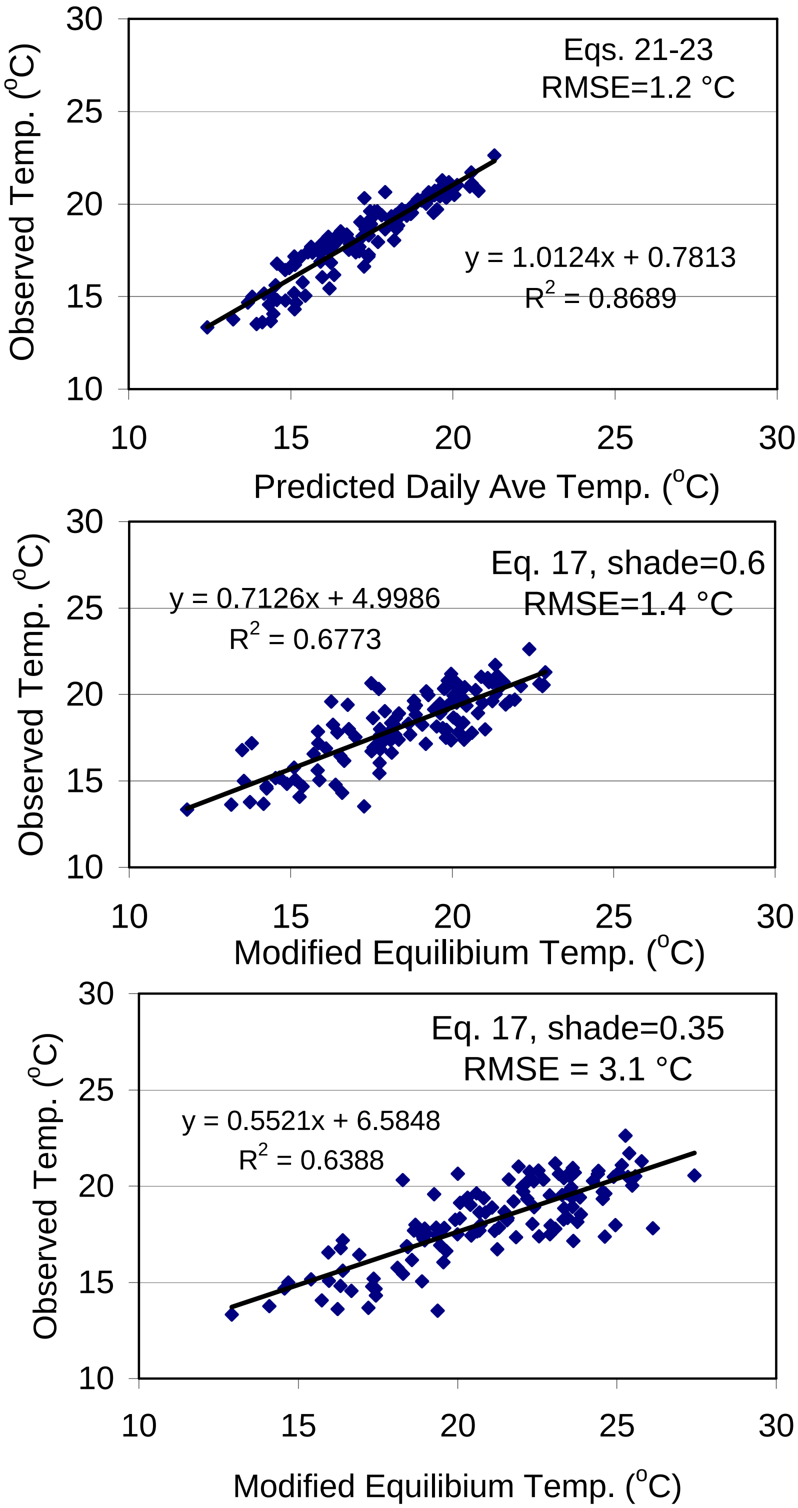

Figure 1.7. Observed daily average stream temperature vs. modified equilibrium temperature from Eq. 17 (lower and center panel) and observed daily average stream temperature vs. daily average temperature from Eq. 21-23 (upper panel) for the USGS stream gaging site on the mainstem, June 1 – September 30, 2008.

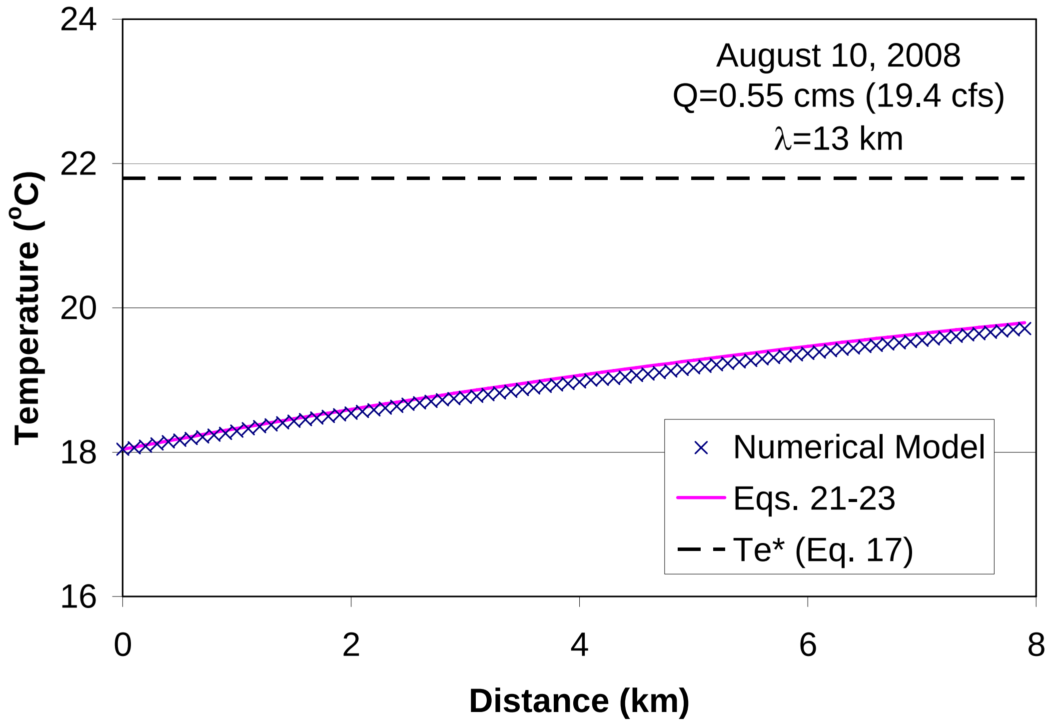

Figure 1.8. Daily average stream temperature vs. distance from the analytic solution (Equations 21-23) and the numerical model for the mainstem reach, August 10, 2008.

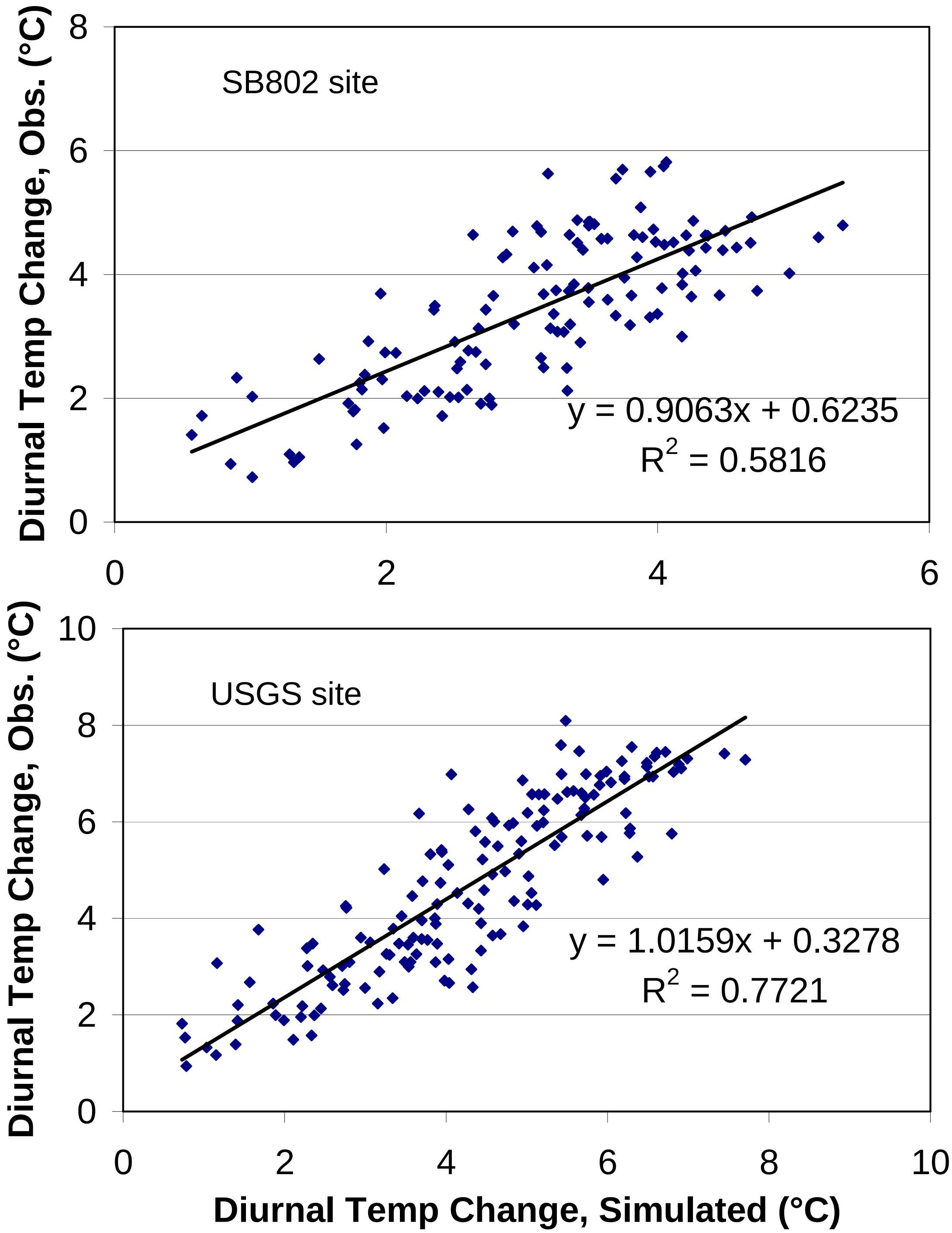

Figure 1.9. Observed vs. predicted diurnal temperature change (δT) from Eq. 29 for the SB802 (upper panel) and the USGS (lower panel) stream gaging stations, June 1 – September 30, 2008. RMSE = 0.9°C and RMSE = 1.0°C, respectively.

1.4. Model Sensitivity Analysis

The analytic modified equilibrium temperature model for mean daily stream temperature and diurnal temperature variations can be used to examine the sensitivity of stream temperatures to hydraulic, riparian and climatic parameters. The sensitivity of the modified equilibrium temperature (T_e*) was investigated for stream reaches with nominal parameters corresponding to the South Branch and mainstem reaches of the Vermillion River summarized in Table 1.4. In all cases, T_e* was calculated using daily climate data for 2008, and averaged over the period June 1 - September 30. Non-temperature parameters were increased by 10%, i.e. multiplied by a factor of 1.1, and the resulting change in modified equilibrium temperature (T_e*) was documented as ΔT^*_e. Temperature parameters (T_g, T_d, T_a) were increased by 1°C above the nominal value. An adjustment to stream discharge (Q) produced corresponding changes to width, based on power law relationships for each reach, while an adjustment to stream width (B) did not affect any other parameters.

For a stream with the characteristics of the South Branch reach, the modified daily equilibrium temperature was found to be most sensitive (Table 1.4a) to the shading coefficient (C_{sh}). A 10% increase in shading produced a stream temperature change ΔT^*_e = - 0.55°C. A change in the groundwater inflow rate or groundwater temperature gave stream temperature changes of ΔT^*_e = - 0.27°C and 0.61°C, respectively. Stream width and average daily air temperature changes gave ΔT^*_e= 0.29°C and ΔT^*_e = 0.56°C, respectively. Sensitivity to stream flow (Q) was found to be small (ΔT^*_e= 0.053°C) and due to the change in stream width with flow. All changes were either a 10% or a 1°C increase in the model input parameter.

Table 1.4a. Mean change (Δ) and standard deviation of change (SD) in three estimated stream temperature response parameters (modified equilibrium temperature =T_e*, diurnal temperature change = δT, and daily maximum temperature = T_{max}, in response to a 10% or a 1°C increase in model input parameter values. Results are calculated changes for the period June 1 to September 30, 2008. Nominal parameter values (T^*_e=15.4°C, δT = 3.0°C, T_{max} = 16.9°C) are for the South Branch reach of the Vermillion River.

Input Parameter (units)	Nominal Value	Modified Value	Response: Mean Change (Standard Deviation), (°C)		
			ΔT^*_e (SD)	$\Delta\ \delta T$ (SD)	ΔT_{max} (SD)
C_{sh}	0.625	0.688	-0.546 (0.219)	-0.344 (0.065)	-0.719 (0.27)
C_{ws}	0.625	0.688	-0.016 (0.05)	0 (0)	-0.016 (0.05)
q_g (L/s/km)	12.7	14.0	-0.273 (0.102)	-0.026 (0.008)	-0.286 (0.101)
T_g (°C)	10.5	11.5	0.61 (0.058)	0 (0)	0.61 (0.058)
Q (m^3/s)	0.339	0.373	0.053 (0.02)	-0.096 (0.015)	0.004 (0.019)
B (m)	3.8	4.1	0.294 (0.11)	0.042 (0.013)	0.315 (0.108)
d (m)	0.23	0.25	0 (0)	-0.208 (0.032)	-0.104 (0.032)
T_a (°C)	20.2	21.2	0.280 (0.05)	0 (0)	0.280 (0.05)
T_d (°C)	13.7	14.7	0.143 (0.042)	0 (0)	0.143 (0.042)

Results were similar for the mainstem reach (Table 1.4b). Considering that a 10% change in shading is ΔC_{sh} = 0.035 for the mainstem reach, but ΔC_{sh} = 0.0625 for the South Branch reach, the sensitivity of T^*_e to shading is similar for the two reaches. The larger stream width of the mainstem (B = 11.2 m versus 3.4 m for South Branch) reduces the sensitivity to groundwater temperature (ΔT^*_e= 0.29°C and 0.61°C, respectively), but increases the sensitivity to air temperature. ΔT^*_e=0.80°C for the mainstem and ΔT^*_e=0.56°C for South Branch.

Table 1.4b. Mean change (Δ) and standard deviation of change (SD) in three estimated stream temperature response parameters (modified equilibrium temperature =T_e*, diurnal temperature change = δT, and daily maximum temperature = T_{max}, in response to a 10% or a 1°C increase in model input parameter values. Results are calculated changes for the period June 1 to September 30, 2008. Stream temperature response (°C) to 10% or 1°C increases in model input parameters. Nominal parameter values (T^*_e= 21.3°C, δT = 4.2°C, T_{max} = 23.5°C) are for the mainstem reach of the Vermillion River.

Input Parameter (units)	Nominal Value	Modified Value	Response: Mean Change (Standard Deviation), (°C)		
			Δ T^*_e (SD)	Δ δT (SD)	Δ T_{max} (SD)
C_{sh}	0.35	0.385	-0.387 (0.159)	-0.19 (0.037)	-0.482 (0.185)
C_{ws}	0.35	0.385	0.102 (0.039)	0 (0)	0.102 (0.039)
q_g (L/s/km)	13.2	14.5	-0.287 (0.117)	-0.006 (0.002)	-0.291 (0.117)
T_g (°C)	10.5	11.5	0.285 (0.056)	0 (0)	0.285 (0.056)
Q (m^3/s)	1.068	1.175	0.022 (0.009)	-0.206 (0.037)	-0.081 (0.035)
B (m)	11.2	12.3	0.29 (0.12)	0.004 (0.003)	0.294 (0.12)
d (m)	0.26	0.29	0 (0)	-0.372 (0.067)	-0.186 (0.067)
T_a (°C)	20.2	21.2	0.402 (0.053)	0 (0)	0.402 (0.053)
T_d (°C)	13.7	14.7	0.255 (0.057)	0 (0)	0.255 (0.057)

The sensitivity of the diurnal stream temperature amplitude (δT) and of the daily maximum stream temperature (T_{max}) to stream morphologic and climate parameters was also explored. Daily maximum stream temperature can be estimated as

$$T_{\max} = T_e * + \frac{\delta T}{2} \qquad (31)$$

Sensitivity analysis results for δT and T_{max} are also summarized in Tables 1.4a and 1.4b. The diurnal stream temperature amplitude δT in the stream reach of the South Branch, was found to be sensitive to shading ($\Delta\delta T$ = - 0.34°C), to stream depth ($\Delta\delta T$ = - 0.21°C), and to stream discharge ($\Delta\delta T$ = - 0.10°C). Diurnal amplitude is notably insensitive to the groundwater inflow rate and groundwater temperature ($\Delta\delta T$ = - 0.026°C and 0, respectively).

The sensitivity of T_{max} to a parameter is the sum of the sensitivity to T_e* and δT. T_{max} was found to be sensitive to shading (ΔT_{max} = - 0.72), groundwater temperature (ΔT_{max} = 0.61), air temperature (ΔT_{max} = 0.56), stream width (ΔT_{max} = - 0.32), and groundwater inflow rate (ΔT_{max} = - 0.29).

The sensitivity of T_e* and T_{max} to groundwater inflow rate (q_g) and shading coefficient (C_{sh}) is illustrated with 2008 climate data in Figure 1.10 for the South Branch reach and Figure 1.11 for the mainstem reach. Calculated time series of T_e* in 2008 are given for varying values of q_g and C_{sh}, keeping other parameters at their nominal values given in Table 1.4a and b. Very low shading or very low groundwater inputs can result in equilibrium temperatures approaching and exceeding 30°C in the South Branch reach and 40°C in the mainstem reach. This is noteworthy because these temperatures substantially exceed temperature tolerances of all trout (salmonid) species. Compared to the South Branch reach, the wider mainstem reach with lower shading requires more groundwater input to reduce stream temperatures.

Figure 1.12 illustrates the tradeoff between stream shading and groundwater inputs to achieve particular values of equilibrium stream temperature. Results are given for temperatures averaged over July, 2008. The groundwater inflow rate is specified as (q_g/B), the average velocity of the groundwater inflow normal to the stream bottom (mm/s). In this way the plot can be applied to streams of any width. However, Figure 1.12 is specific for July 2008 climate and groundwater temperature of 10°C and 12°C.

Figure 1.13 gives information on the relationships between stream shading, groundwater inputs, and stream temperatures in a slightly different form compared to Figure 1.12. Stream equilibrium temperature is plotted against shading for lines of constant groundwater input velocity (q_g/B). Plots are given for mean climate conditions in July and September in the Twin Cities area, with July stream temperatures substantially higher for the same shading and groundwater inputs. Note that for higher groundwater input rates, stream temperature is less sensitive to changes in shading. If groundwater inputs for a stream reach are considered fixed, the effect of riparian shading management on stream temperature can be easily found using such a figure.

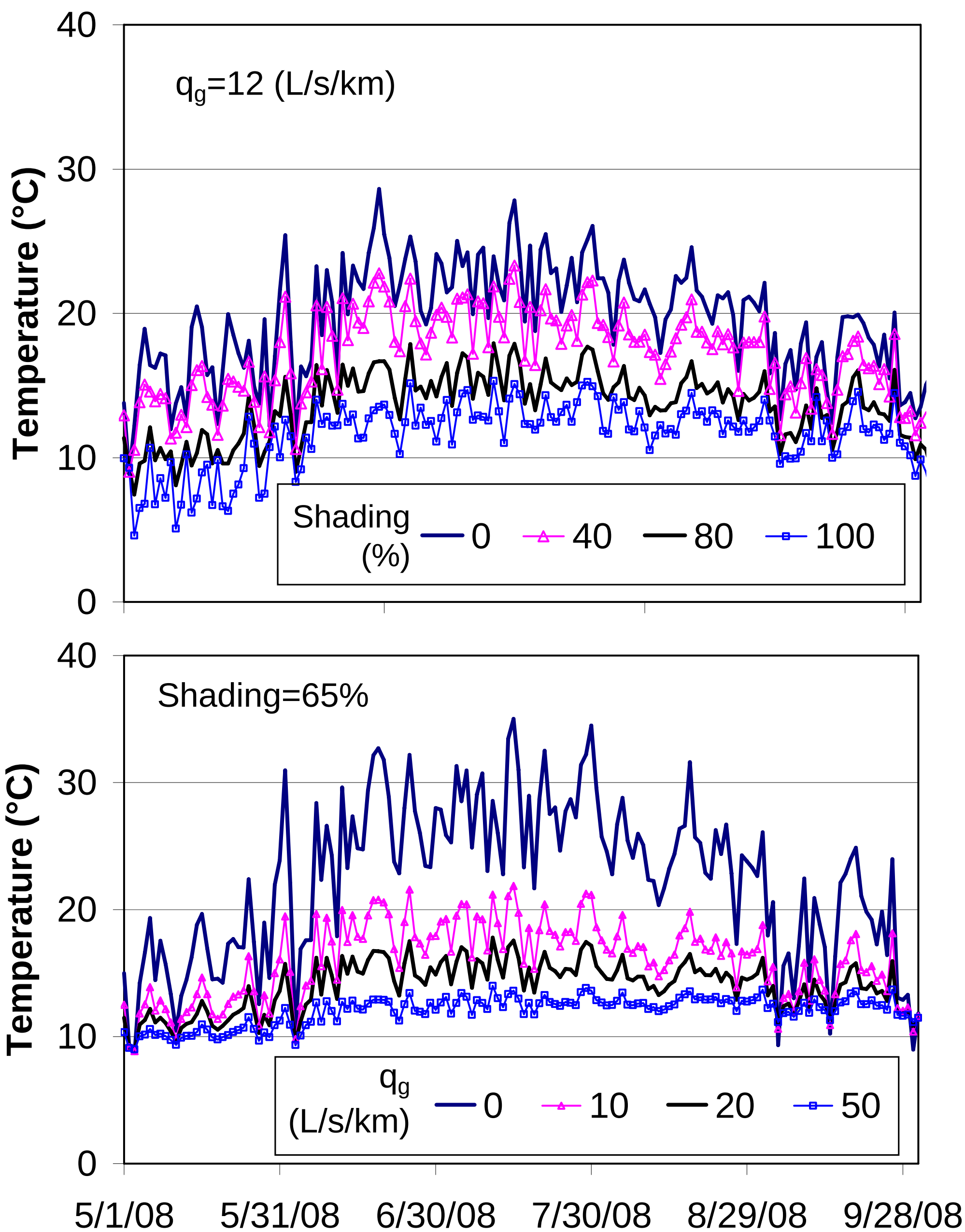

Figure 1.10. Sensitivity of daily adjusted equilibrium temperature (T_e*) to the shading coefficient (upper panel) and groundwater inflow rate (lower panel) for the South Branch reach (*B*=3.7m) and 2008 climate data. The wind sheltering coefficient was set equal to the shading coefficient in all cases.

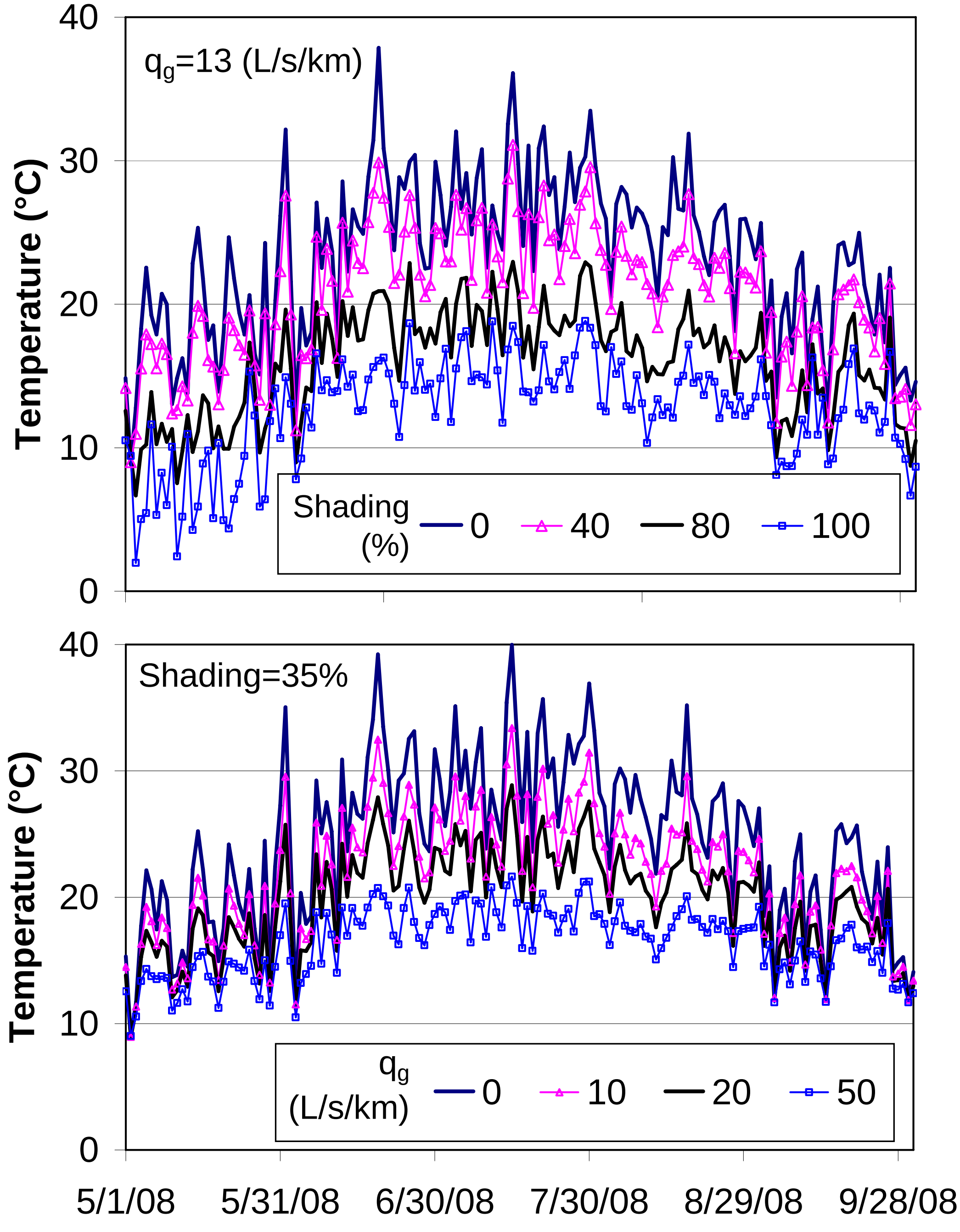

Figure 1.11. Sensitivity of daily adjusted equilibrium temperature (T_e*) to the shading coefficient (upper panel) and groundwater inflow rate (lower panel) for the mainstem reach (B = 11.2m) and 2008 climate data. The wind sheltering coefficient was set equal to the shading coefficient in all cases.

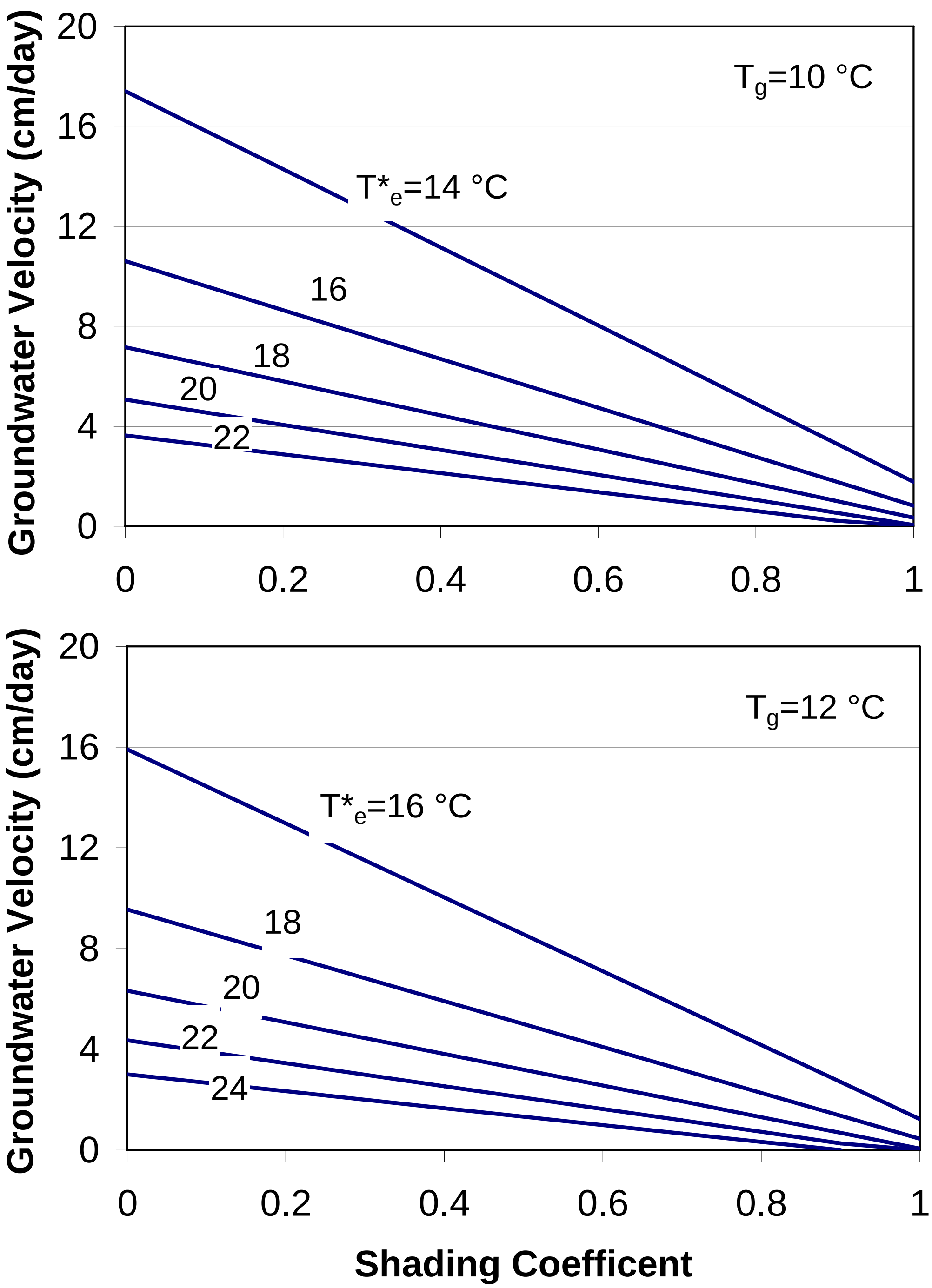

Figure 1.12. Equilibrium temperature (T_e*) isotherms in a plot of groundwater inflow velocity (q_g/B) vs. shading coefficient. All temperature values are averaged over July, 2008. Groundwater inflow temperatures are T_g = 10°C (upper panel) and T_g = 12°C (lower panel).

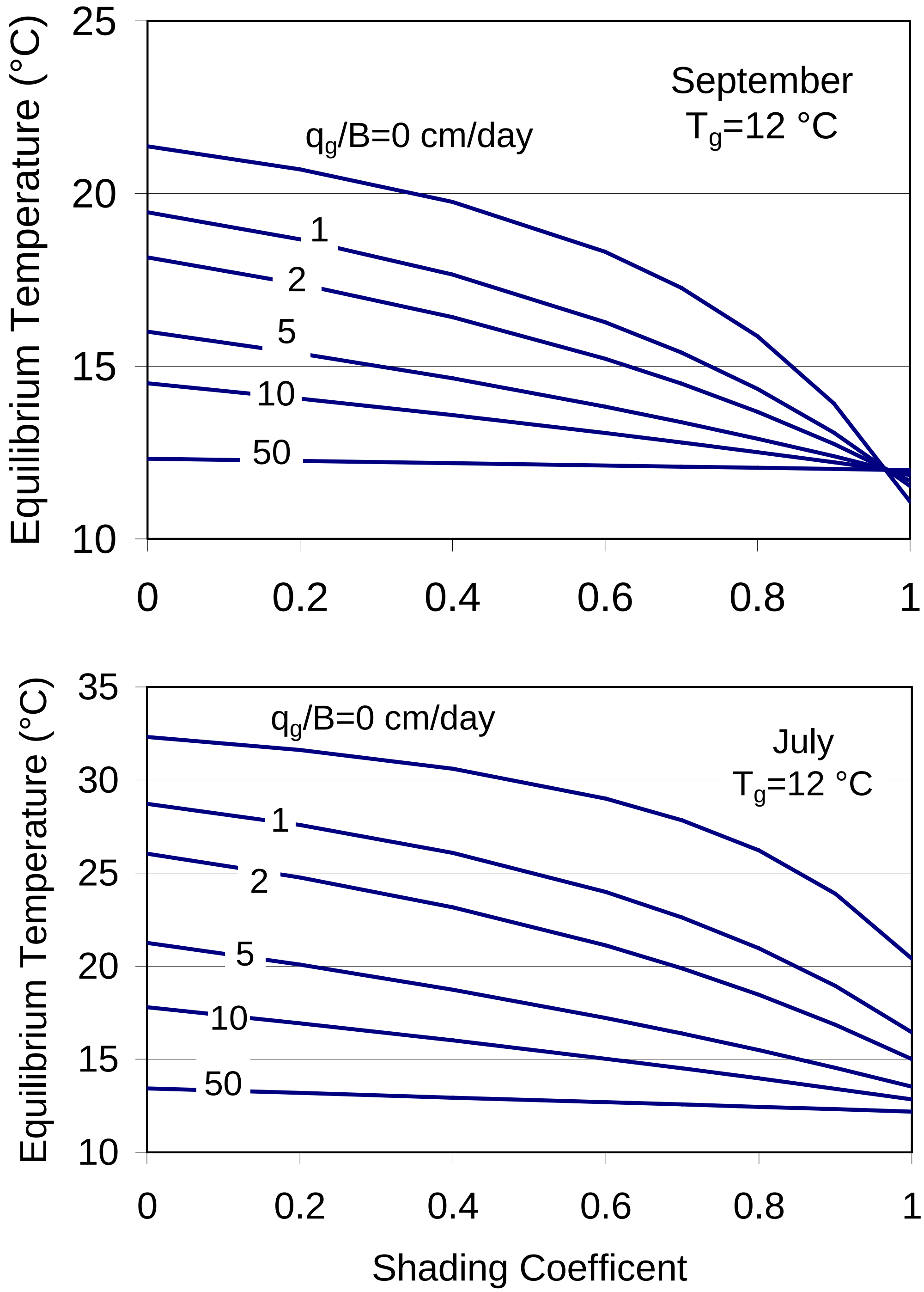

Figure 1.13. Equilibrium temperature versus shading and groundwater inflow velocity for averaged climate in July 2008 (lower panel) and September 2008 (upper panel). Groundwater inflow temperatures is $T_g = 12$°C.

1.5 Summary and Conclusions (Part I)

The temperature of a coldwater stream depends on the balance of the heat fluxes across the water surface (short and long wave radiation, convection and evaporation) and the heat fluxes across the sediment surface (groundwater inflow and conduction to the sediment). Previous equilibrium temperature models have reduced the complex heat transfer across the water surface to a net transfer rate that depends on a bulk heat transfer coefficient (K) and a temperature difference between the water and the equilibrium temperature [*Edinger et al.* 1968]. A modified (extended) equilibrium temperature (T_e*) model for coldwater streams has been developed and tested. The new model adds a second bulk coefficient (K_s*) and the streambed temperature (T_g) to modulate the influence of the groundwater inflow and sediment temperature on stream temperature.

For small, groundwater-fed streams, the surface and subsurface heat transfer coefficients, K and K_s^*, respectively, can be of similar magnitude. For a given rate of groundwater input (flow rate per unit stream length), the degree of influence of groundwater on stream temperature scales inversely with stream width, so that a given groundwater inflow (flow/length) will have less impact on stream temperature for wider streams. Typical trends of increasing stream temperature with downstream distance observed in field studies of trout streams [*Caissie* 2006] can be attributed to a combination of this groundwater effect and the typical reduction in riparian shading as channel width increases.

The modified equilibrium temperature model for coldwater streams formulated and used in this study gives an upper bound for daily average temperature based on climate conditions, riparian shading, stream width, and groundwater inputs. Two reaches of the Vermillion River were successfully modeled in this study. For streams with non-uniform shading due to development or other factors, riparian shading needs to be averaged over appropriate length scales for equilibrium conditions. For the main stem of the Vermillion, this length scale was estimated with Equation 23 as 20 km.

The amplitudes of diurnal temperature fluctuations of streams depend on the daily solar radiation and air temperature cycles, and can be estimated with relatively simple analytic models. The diurnal temperature variation also depends on stream depth, since depth determines the thermal mass of water per unit surface area. Groundwater inflows to a stream were found to have relatively little effect on diurnal temperature variation in the two stream reaches studied. Hyporheic exchange flows can have a measureable influence on diurnal temperature changes in streams with alluvial substrates because they increase the mass of water to be heated and cooled in the diurnal cycle increase, similar to stream depth [*Burkholder* 2008; *Story et al.* 2003]. Hyporheic exchange flows were not included in the modified equilibrium temperature model, because they depend on morphological features such as permeability of the stream bed [*Burkholder* 2008]; stream depth can, however, be considered as a surrogate for hyporheic effects. The equilibrium temperature and diurnal temperature variation models were combined to give an estimate of daily maximum stream temperatures.

A sensitivity analysis of the equilibrium temperature model confirms that water temperatures in coldwater streams vary strongly with riparian shading, stream width, and both groundwater inflow rate and temperature. While increased wind sheltering can reduce evaporative (latent) and convective (sensible) heat fluxes, the sensitivity of stream temperature to wind sheltering was found to be an order of magnitude lower than the sensitivity to shading changes. This result is in agreement with previous studies showing that convective/evaporative heat fluxes tend to be smaller than radiation fluxes [e.g. *Johnson* 2004].

The decreased sensitivity of stream temperature to air temperature for streams with larger groundwater inputs predicted in this study is in qualitative agreement with previous studies [*Caissie* 2006]. However, groundwater-fed stream reaches will be sensitive to increases in groundwater temperature, which can be expected to rise with mean annual air temperature. The models developed in this study provide a convenient means to estimate the stream temperature–air temperature slope, and are appropriate for studying the regional response of stream temperature to climate change.

The modified equilibrium temperature model is applicable to the study of specific coldwater stream reaches. Benefits of additional riparian shading or changes in stream morphology can be explored (simulated) with the model before management decisions are made. Trends in daily average and daily maximum stream temperatures in the warmest months can be studied with a minimum of in-situ stream geometry and flow data, yet the model is fairly realistic and allows for extrapolations because it is built on deterministic relationships. Basic information such as the shading-groundwater relationships given in Figure 1.12 can be used to quantify the importance of riparian cover and groundwater inputs in maintaining acceptable stream temperatures. The stream temperature model can be run with input provided by GIS analysis tools. Smaller stream systems may require aerial imagery for stream geometry and riparian shading, when satellite imagery has insufficient spatial resolution. Further work is needed to build data bases of coldwater stream morphology and hydrology and to estimate groundwater inputs so that the coldwater stream temperature projection tool developed in this study can be applied at a regional scale.

Part II. Projected impact of climate change on coldwater stream temperatures in Minnesota: Model simulations

2.1 Introduction

Coldwater fish species such as trout are found only in streams that meet certain temperature criteria because water temperature regulates the rates of biological and chemical processes, and is therefore an important aquatic habitat parameter (Eaton *et al.* 1995). The water temperature in streams and rivers is usually controlled by surface heat transfer processes with the atmosphere (Edinger *et al.* 1968, Sinokrot and Stefan 1993). Coldwater reaches of streams typically have substantial riparian shading and are fed by a cold water source, e.g. groundwater, deep reservoirs, ice- or snowmelt-water, or wetlands. Long term climate change, particularly increases in air temperature, is expected to lead to increases in stream and river water temperatures because of its direct effect on the heat transfer processes on the water surface. Stream temperature increases due to climate change may impact coldwater fish populations through a number of mechanisms, including metabolic changes, decreases in dissolved oxygen and increased uptake of contaminants (Ficke *et al.* 2007). Streams that are already impacted by land development may be particularly susceptible to climate changes (Webb *et al.* 2008). A second effect which has received relatively little attention is the warming of the source waters due to climate change (Meisner 1988). This dual effect of climate change on stream temperature will be investigated in this paper for Minnesota coldwater streams and climate conditions.

The change in stream temperatures due to climate and land use changes has been estimated using both empirical and deterministic models (Caissie 2006; Hari *et al.* 2006; Nelson and Palmer 2007; Webb *et al.* 2008). Deterministic, numerical stream temperature models can be used to predict the temperature response of a specific stream to climate change (Kim and Chapra 1997; Sinokrot and Stefan 1994). Such models require a substantial input of weather and stream parameters to quantify the different heat transfer processes. Stream-specific or regional regression models can also been created to study the impact of climate change on stream temperature (Clark *et al.* 2001; Mohseni *et al.* 1999). Stream temperature – air temperature regression models that characterizes stream temperature for past conditions can give the sensitivity of stream temperature to air temperature (e.g. Stefan and Preud'homme, 1993; Webb *et al.* 2003) , which in turn can be used to estimate future stream temperature from air temperature projected by global climate models (Erickson and Stefan 2000; Mohseni and Stefan 1998, 1999, Morrill *et al.* 2005). These regression models characterize the response of stream temperature to atmospheric heating using air temperature as a surrogate, but do not take into account long term changes in source water, e.g. groundwater temperatures in response to air temperature changes.

If equilibrium temperature (Edinger *et al.* 1968) is used as the independent variable instead of air temperature, the atmospheric heat transfer components are more explicitly taken into account in the projection of the stream temperature response to climate change (Bogan *et al.* 2003). However, equilibrium temperature or air temperature alone are not necessarily good predictors of stream temperature, especially coldwater streams because surface and subsurface water and heat inputs of source water can contribute significantly to a coldwater streams heat budget (Bogan *et al.* 2004).

Previous research on the effects of climate change on stream temperature has focused on atmospheric heat transfer components and ignored source water input. For many coldwater stream reaches in Minnesota that input is crucial in summer to maintain moderate temperatures. Soil and groundwater temperatures can be expected to increase with long term air temperature increases (Meisner *et al.* 1988), providing an additional mechanism for stream temperature response to climate change. Wetland systems acting as a water source for streams can also be expected to increase in temperature. In this paper, a previously developed stream temperature model based on equilibrium temperature is used to assess the response of stream temperature to climate change scenarios, taking into account both changes in atmospheric heat transfer and source water temperature. Two wetland-fed, coldwater trout streams near Duluth, MN and a groundwater-fed coldwater trout stream south of Minneapolis/St. Paul, MN are considered. The response of each stream to climate change is assessed in terms of 1) changes in direct atmospheric heat transfer to the stream, 2) changes in the temperature of water sources (groundwater, wetlands) and 3) the combined effects of changes in both atmospheric heat transfer and source temperatures.

2.2 Study Sites

The three study streams include an example of a groundwater-fed coldwater stream south of Minneapolis/St. Paul, MN (South Branch of the Vermillion River) and examples of two wetland-fed streams in Duluth, MN (Miller Creek and Chester Creek). The locations of the three sites are shown in Figure 2.1. South Branch, Miller Creek, and Chester Creek have watershed areas of 84, 24, and 18 km^2, respectively. All three are designated trout streams.

The Vermillion River flows through a relatively flat region covered by several major glacial moraines. The watershed is mostly made up of glacial drift from two separate glacial advancements (Superior and Des Moines lobes). The Vermillion River receives groundwater discharge from a quaternary surface aquifer that has a typical thickness from 7 to 35 m. There are also localized connections to two deeper aquifers – the Prairie du Chien and Jordan aquifers. The river sits in buried valleys filled with sand and gravel with high hydraulic transmissivity and recharge potential near the stream (EOR, 2007; Erickson and Stefan, 2009), and in particular, near portions of the river that are designated trout stream, including portions of South Branch. Although the Vermillion River watershed has some areas of increasing residential and commercial development, the study area (South Branch) has primarily agricultural land use (78%).

Miller Creek and Chester Creek have hydrogeologic features typical of streams in the Duluth area and northeastern Minnesota. The upper watersheds are relatively flat, covered with thin glacial deposits (Fitzpatrick *et al.* 2006), and with prominent wetland areas. Lower sections of the watersheds have steep slopes, very little soil coverage and are confined or entrenched valleys carved through bedrock. Groundwater storage is not well characterized, but it is believed that wetlands in the upper portions of the watersheds provide most of the hydrologic storage. Miller

Creek, in particular, has been impacted by development, with historical wetland loss and increased impervious surface area, currently about 23%.

Substantial temperature and flow monitoring has occurred on the Vermillion River over several years, and numerical models for stream flow and temperature have been developed (Herb *et al.* 2008a, b). For the present study, South Branch, a tributary of the Vermillion River, was selected (Figure 2.1). Water temperature has been monitored in stream reaches in 2006, 2007, and 2008. The 2008 data were used in this study to calibrate a stream temperature model, because additional parameters related to groundwater inputs were measured in 2008. Continuous 15-minute stream flow data for 2008 were obtained for the AES-21 (SB802) site on the South Branch of the Vermillion River (Figure 2.1). Representative stream temperature data for the South Branch was obtained from the Klaus monitoring station (Figure 2.1). Stream temperature was monitored by the Dakota County Soil and Water Conservation District and the Minnesota Department of Natural Resources using Onset Hobo temperature loggers. 2008 climate data for the South Branch stream temperature model calibration were available from the Airlake Airport near Lakeville, including air temperature, humidity, and wind speed at 1-hour interval. 10-minute solar radiation data were recorded at the St. Anthony Falls Laboratory, University of Minnesota, in Minneapolis, approximately 30 km north of the Vermillion River. For climate change analysis, a longer time record was obtained for the Minneapolis/St. Paul International Airport, which is about 25 km north of South Branch. This data set includes simulated solar radiation and was obtained for the period 1961-2005 from the National Renewable Energy Laboratory (NREL) (http://rredc.nrel.gov/solar/old_data/nsrdb/).

Substantial stream temperature monitoring data was also available for Miller Creek, in Duluth, MN (Figure 2.1), including sites in the main stem, tributaries, and stormwater inlets. Stream temperature data was taken by the South St. Louis Soil and Water Conservation District, mainly using Onset Tidbit temperature loggers. Flow data (1-hour) was available from a gaging station near the outlet of Miller Creek (Figure 2.1) for 1997, 1998, 2007, and 2008. Stream temperature and discharge data for Chester Creek were obtained from the Duluthstreams web site <www.duluthstreams.org>. Climate data for the Duluth area streams was obtained from Duluth International Airport, which is at the upper end of the Miller Creek watershed. For 2008 only, 1-hour observed solar radiation data were obtained from the Minnesota Pollution Control Agency from a station in the lower portion of the Miller Creek watershed. For other years (1961-2005), simulated hourly solar radiation data were obtained from the NREL for Duluth International Airport.

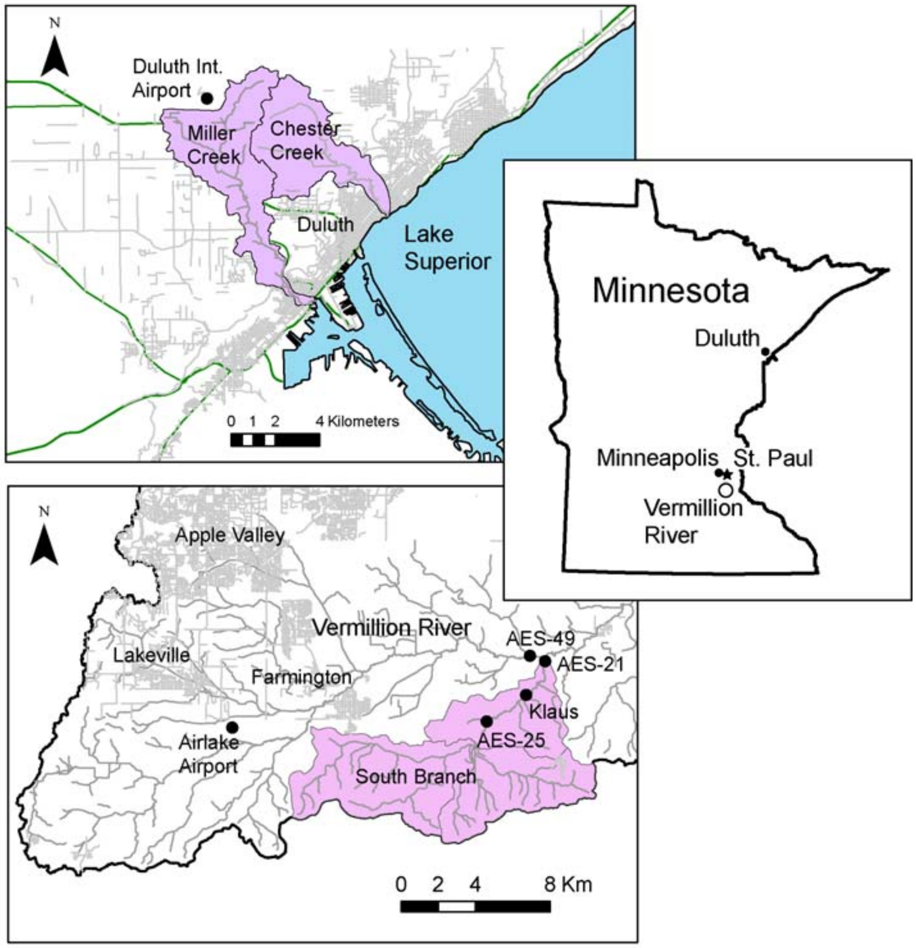

Figure 2.1. Study streams in Duluth, MN (Miller Creek, Chester Creek) and south of Minneapolis/St. Paul (Vermillion River).

2.3 Source Water Temperatures

2.3.1 Wetland temperatures

The North Shore region of Lake Superior in Minnesota has over 100 designated trout streams. This region does not have large groundwater aquifers, due to the presence of shallow and surface bedrock. Wetlands and lakes are a significant source of hydrologic storage in these watersheds (Detenbeck *et al.* 2003). Very little information is available on the storage characteristics of the North Shore wetland systems, other than what can be discerned from observed stream discharge. Comparison of hydrographs from streams in the Duluth, MN area to a similarly sized tributary of the Vermillion River, south of Minneapolis/St. Paul, MN clearly shows the relative lack of hydrologic storage in the North Shore systems (Figure 2.2).

Visual inspections of the wetlands in the Miller Creek watershed show relatively little standing surface water and surface channelization connecting the wetlands to the stream channel of Miller Creek. As a result, it is assumed that much of the connection between wetlands providing hydrologic storage and the stream channel is mainly by subsurface flow.

Source water temperatures for the Duluth area streams were obtained from 1) several years of monitored temperatures in wetland (standing) water in the Miller Creek watershed at Ridgeview Rd and 2) a previously developed computer model for the temperature of surface and subsurface water in wetlands (Herb *et al.* 2007). The model includes the effect of emergent vegetation on surface heat transfer processes. Using observed climate data from the Duluth International Airport, the wetland model was able to reproduce the observed surface water temperature time series (Figure 2.3) with a root-men-square error (RMSE) =1.4ºC. The primary calibration parameter for the wetland temperature model is a vegetation density parameter which varies from 0 to 1 and impacts shading and evaporation. For the Duluth wetland simulations, a relatively high vegetation density parameter (0.95) was determined by temperature calibration.

Simulated (or observed) wetland temperatures used as a source temperature for stream temperature simulations tended to give an excessive response of stream temperature to weather (climate) parameters when used at a daily time scale. Better results were obtained by using, e.g. a 7-day running average of wetland temperature or a second order polynomial fit of the seasonal variation of wetland temperature as the source temperature. A polynomial fit of the 10-year average (1997-2005, 2008) simulated daily wetland temperature also produced good stream temperature simulation results for 2008 data (Figure 2.4). The maximum summer source water (wetland) temperatures are reached at the end of July, approximately. The 10-year average source temperature was subsequently used for all simulations of Duluth-area streams, because it gives good temperature simulation results for current conditions and provides a good basis for estimating future source temperatures for these systems.

To specify climate change, Duluth climate data (1997-2005, 2008) was incremented using two future climate scenarios (GCMM 2.0 and 3.1 described in Section 2.5), and the wetland temperature model was also run for these scenarios. In addition to running incremented future climate scenarios above the wetland, the soil temperature at the lower boundary of the wetland model (10 m into the ground) was incremented by the projected change in mean annual air temperature for the region (5.0ºC for CGCM 2.0, 4.0ºC for CGCM 3.1). The projected change in wetland source water temperature with average increments of 2.7ºC and 3.5ºC and maximum increments of 4.3ºC and 3.2ºC for CGCM 2.0 and 3.1, respectively. These temperature increments are lower than the specified air temperature increments during the summer months, mainly due to evaporative cooling.

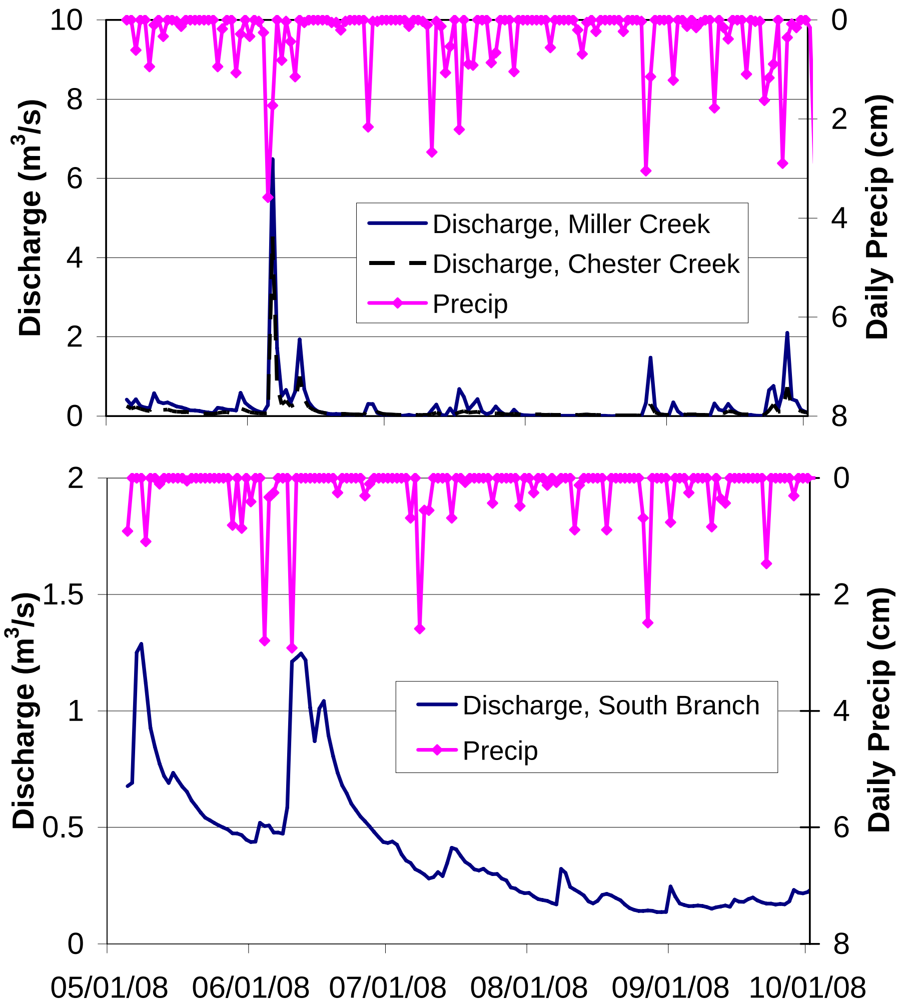

Figure 2.2. Precipitation and stream discharge timeseries for two North Shore trout streams in Duluth, MN (Miller and Chester Creek), and a groundwater-fed trout stream south of Minneapolis/St. Paul (South Branch of the Vermillion River).

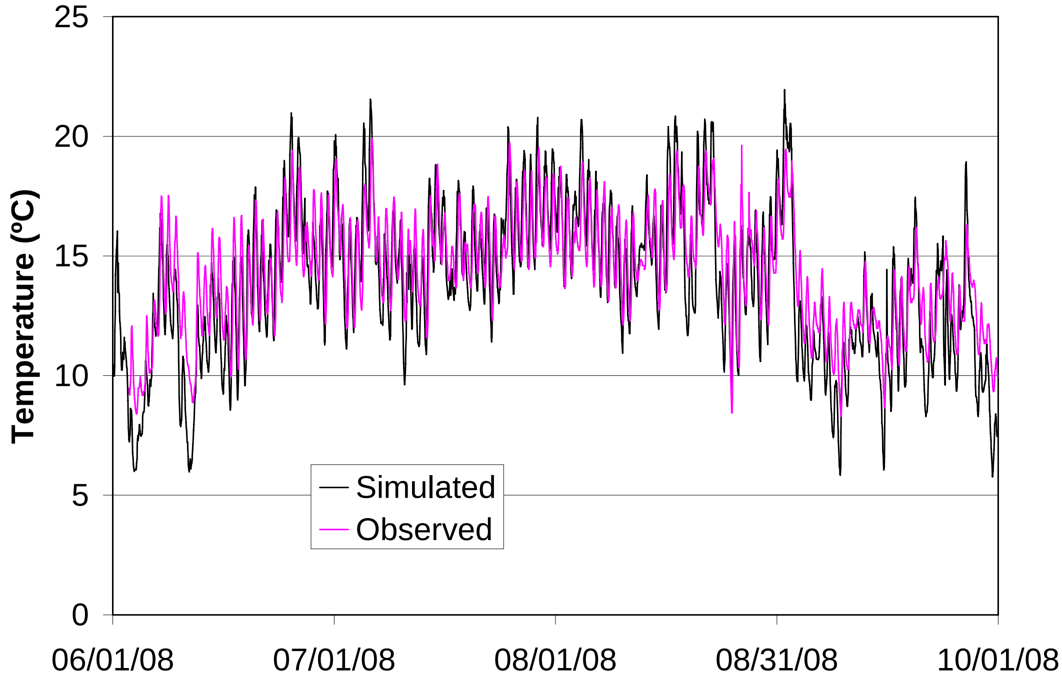

Figure 2.3. Simulated and observed wetland temperatures for the Ridgeview Rd. monitoring point in 2008. The simulations are at a 1-hour time step and have an RMSE = 1.4ºC.

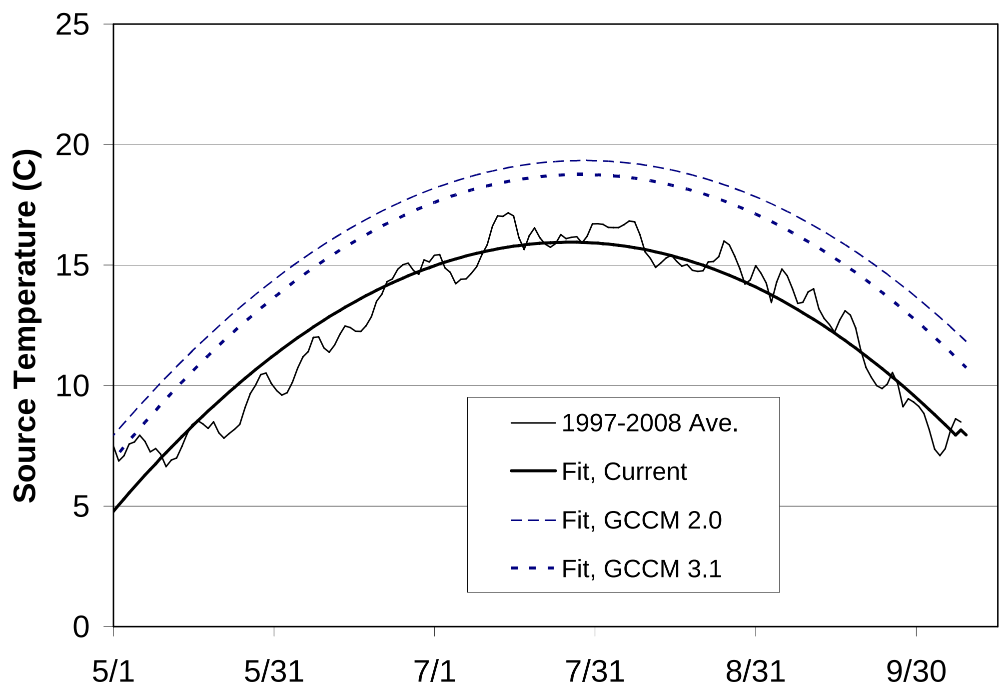

Figure 2.4. Simulated source water (wetland) temperatures for current conditions (average of 1997-2005, 2008) and for the CGCM 2.0 and 3.1 climate scenarios.

2.3.2 Groundwater temperatures

Groundwater temperatures depend on the depth of the aquifer. Water temperatures in shallow aquifers in Minnesota, down to depths on the order of 10m, respond to seasonal temperature changes on the ground surface; amplitudes and lag times vary with depth (Taylor and Stefan 2009). Groundwater from deep aquifers is isothermal year around. Its temperature is imposed by the long-term (multi-year) average ground surface temperature.

The Vermillion River is an example of a groundwater-fed Minnesota trout stream. Direct measurements of source water (groundwater) temperatures were available from 1) temperature measurements in the streambed of gaining stream reaches, i.e. stream reaches that receive groundwater, and 2) temperature measurements in several shallow groundwater wells in the watershed. Streambed temperatures were monitored at a depth of about 40 cm into the sediment bed using piezometers equipped with Onset Hobo temperature loggers. The monitoring work was installed and operated by Applied Ecological Services, Inc. in St. Paul, MN. Examples of streambed temperatures plotted in Figure 2.5 show that the AES-21 site had a constant streambed temperature, suggesting that the groundwater came from a depth where temperatures are unaffected by seasonal changes; the constant 9°C temperature is close to the 7.4°C mean annual air temperature in the Twin Cities area. The streambed temperatures at sites AES-25 and A-49 varied by several degrees over the summer period, and reached maximum values from August to September (Figure 2.5).

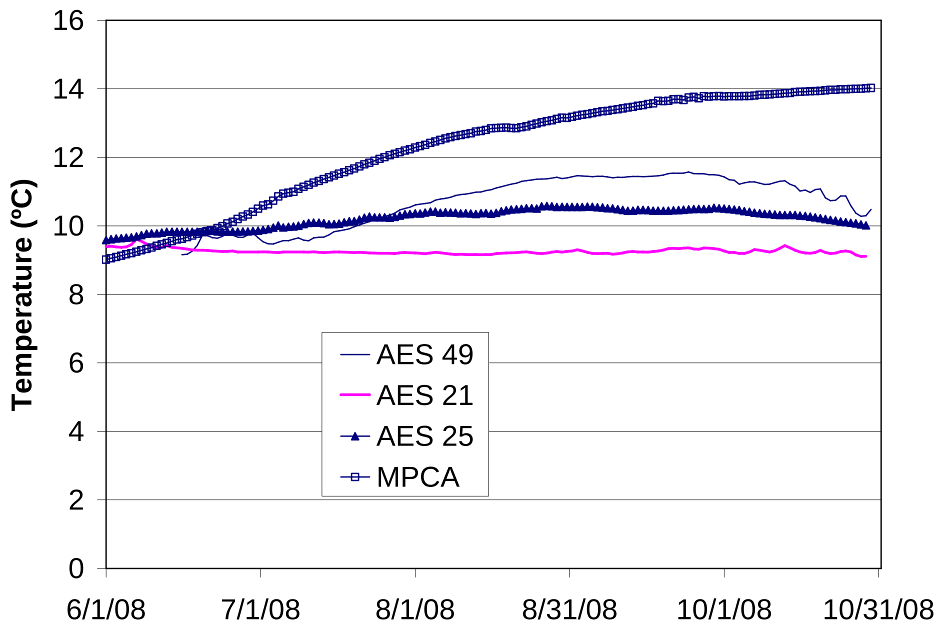

Figure 2.5. Observed streambed temperatures at 3 sites (AES 21, 25, 49) in the Vermillion River and observed temperature from a shallow groundwater well (MPCA). The locations of the sites are shown in Figure 2.1.

Shallow groundwater temperatures from 3m depth in a well in Farmington, MN, were obtained from the Minnesota Pollution Control Agency. The seasonal temperature excursion is 5^{o}C, and a maximum temperature is reached in October.

Using the various streambed temperatures as source water temperatures, the AES 49 site temperature gave the best prediction of stream temperature at the South Branch site as will be shown in a later section. To project an increase in source water (groundwater) temperature due to climate change, the observed 2008 groundwater temperature was incremented by the projected change in mean annual air temperature (5.0ºC for CGCM 2.0, and 4.0ºC for CGCM 3.1) for the future climate scenarios.

2.4. Stream Temperature Model Calibration and Sensitivity

2.4.1 Stream temperature model calibration

The modified equilibrium stream temperature model described in Part I of this report was applied to simulate daily summer temperatures in the three study streams. Individual models were calibrated for the South Branch of the Vermillion River, for Miller Creek, and for Chester Creek using recorded time series of source temperatures described in Section 2.2. The calibration parameters were the shading and wind sheltering coefficients, and the source water (groundwater) inflow rate (q_g) and source water (groundwater) temperature (T_g). These calibration parameters were varied to achieve the lowest root-mean-square error (RMSE) between the predicted daily stream temperatures and the observed daily stream temperatures for June – September 2008. In addition, the slopes and intercepts of the air temperature – stream temperature relationships were compared for simulated and observed stream temperatures, to ensure that the model was correctly predicting the response of stream temperatures to air temperature variations. The stream width was calculated for each day based on the observed stream discharge using a power law relationship. The calibration parameter values, and the RMSE statistics are summarized in Table 2.1. The stream temperature simulations had an RMSE close to 1°C for all three streams, which is typical for stream temperature simulations. The simulated and observed daily stream temperatures are plotted in Figures 2.6 and 2.7 for Miller Creek and South Branch, respectively.

Table 2.1. Stream temperature model fit parameters.
The groundwater inflow rate is given in units of liters/second/kilometer.

	Shading coeff. C_{sh}	Sheltering coeff. C_{ws}	GW inflow rate q_g (l/s/km)	RMSE (°C)
Miller	0.59	0.59	11.8	1.04
Chester	0.60	0.60	14.7	1.02
South Branch	0.50	0.50	13.0	0.90

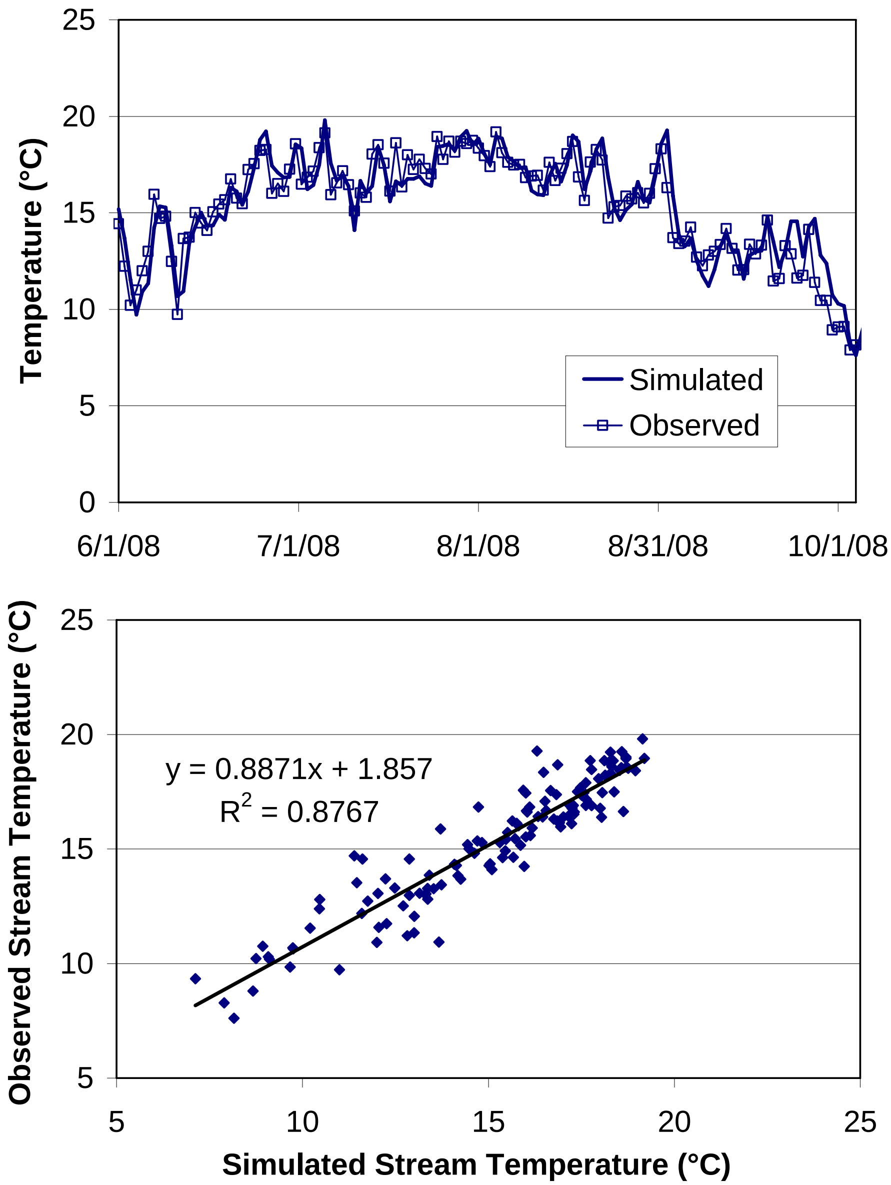

Figure 2.6. Time series of simulated and observed daily average stream temperature (upper panel) and observed vs. simulated daily average stream temperature (lower panel) for Miller Creek, June – September 2008.

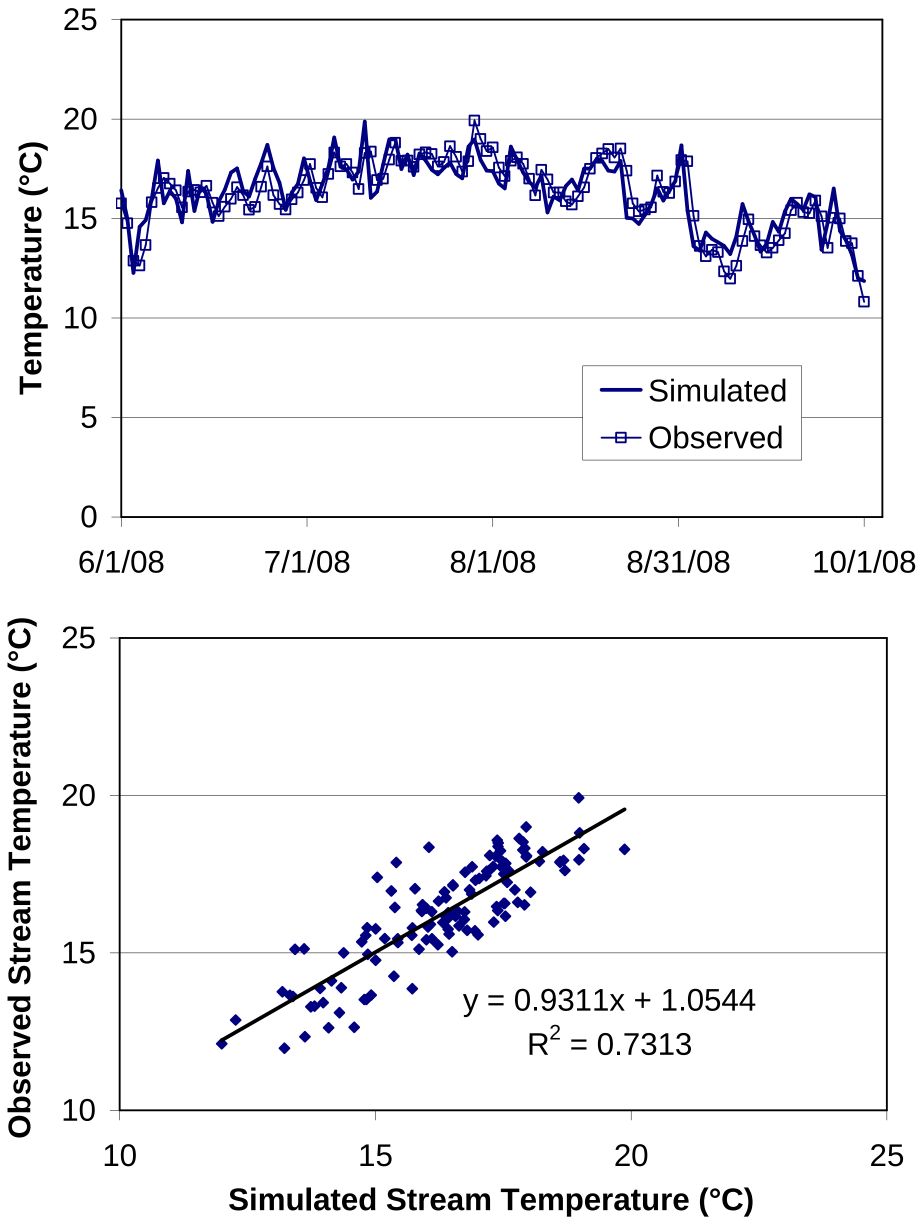

Figure 2.7. Time series of simulated and observed daily average stream temperature (upper panel) and observed vs. simulated daily average stream temperature (lower panel) for South Branch, June – September 2008.

2.4.2 Stream temperature sensitivity to air temperature

The response of stream temperatures to climate change is mainly driven by changes in air temperature. The slope and the intercept of the linearized stream temperature – air temperature relationship are therefore important elements of stream temperature projection. An example of these relationships for observed data and simulated values is given in Figure 2.8 for Miller Creek. The slopes and intercepts of the linearized air temperature – stream temperature relationships are summarized in Table 2.2 for all three streams. In general, the simulated daily stream temperatures tended to give slightly higher slopes and slightly lower intercepts with air temperature compared to observed stream and air temperatures. The level of agreement of these slopes and intercepts between simulated and observed stream temperature was used to determine the most appropriate seasonal variation of source temperatures (see Section 2.3)

Table 2.2. Stream temperature vs. air temperature relationships for Miller Creek, Chester Creek, and South Branch for observed and simulated stream temperatures.

	Observed		Simulated	
	Slope	Intercept (^oC)	Slope	Intercept (^oC)
Miller	0.60	5.8	0.65	4.9
Chester	0.43	7.6	0.45	7.2
South Branch	0.43	7.6	0.44	7.2

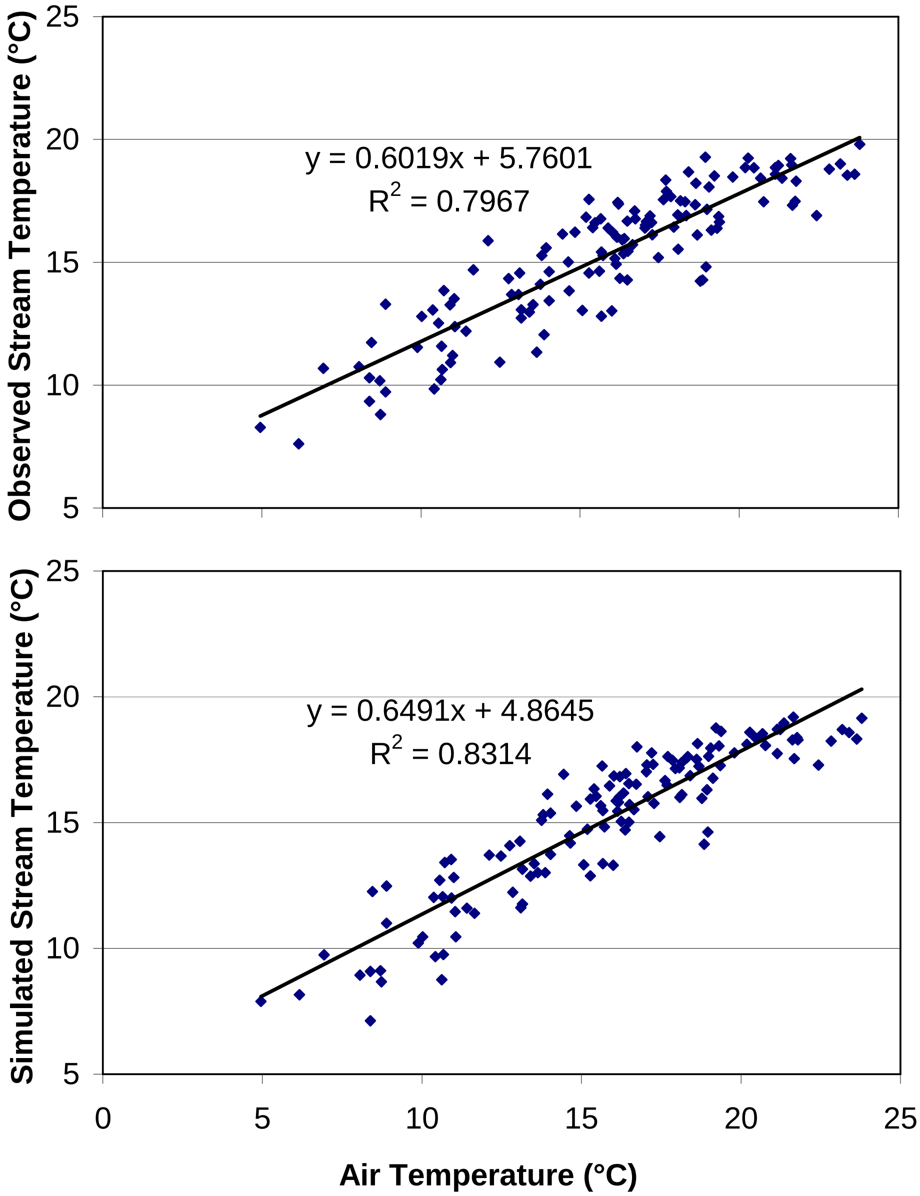

Figure 2.8. Observed (upper panel) and simulated (lower panel) daily average stream temperature vs. observed daily average air temperature for Miller Creek, June – September 2008.

2.5 Climate Change Scenarios

Climate change scenarios from the Canadian Centre for Climate Modeling were used. Two scenarios were used: the 2xCO2 doubling scenario from the CGCM version 2.0 model results, and the A1B scenario (rapid economic growth) from the CGCM version 3.1 results. The CGCM version 2.0 was selected to allow direct comparisons to previous fish habitat studies for Minnesota (e.g. Mohseni *et al.* 1999), while the CGCM 3.1 version includes more recent results with higher spatial resolution. Climate parameters for both scenarios were downloaded from the Intergovernmental Panel on Climate Change (IPCC) data center. Monthly average increments to air temperature, humidity, solar radiation, cloud cover, and precipitation were calculated for the spatial model nodes closest to Duluth and Minneapolis/St. Paul, MN. The climate parameter increments were calculated and provided by Prof. Xing Fang, Dept. of Civil Engineering, Auburn University. The monthly increments for each scenario and climate parameter are summarized in Tables 2.3 to 2.5.

Table 2.3. Monthly increments of climate parameters for Minneapolis and Duluth, MN from scenario CGCM 2.0. (+) indicates an additive increment, (x) indicates a multiplicative factor.

Month	Air temp T_a (°C) (+)	Spec.humidity q (x)	Solar rad. h_s (x)	Wind speed W_o (x)	Precipitation (x)
1	8.17	1.85	0.94	1.08	1.23
2	8.50	1.94	0.92	1.10	1.26
3	4.37	1.53	0.95	0.88	1.22
4	5.76	1.78	0.95	1.01	1.50
5	5.39	1.46	0.97	0.97	1.05
6	4.27	1.32	0.96	0.85	0.99
7	3.54	1.23	0.96	0.80	0.87
8	5.24	1.35	0.99	0.83	0.87
9	4.51	1.29	0.99	0.90	0.79
10	2.71	1.19	0.98	1.01	0.96
11	2.90	1.29	1.01	1.02	0.96
12	4.38	1.25	1.00	0.91	0.97
Average	4.98	1.46	0.97	0.95	1.06

Table 2.4. Monthly increments of climate parameters for Minneapolis, MN from scenario CGCM 3.1. All increments are additive (+), with indicated units.

Month	Air temp T_a (°C)	Relative Humidity RH	Solar rad. h_s (W/m^2)	Wind speed W_o (m/s)	Precipitation (cm)
1	4.84	0.0009	-3.63	0.53	0.021
2	8.09	0.0011	-18.51	0.43	0.055
3	6.25	0.0010	-26.67	0.17	0.053
4	3.60	0.0011	-12.59	0.71	0.038
5	3.47	0.0015	-9.67	0.57	0.043
6	3.28	0.0019	1.10	0.46	-0.023
7	3.25	0.0022	7.16	0.21	-0.029
8	3.32	0.0022	1.77	0.34	-0.026
9	3.34	0.0020	0.17	0.17	-0.007
10	3.39	0.0016	-0.57	0.37	0.027
11	3.06	0.0011	-1.05	0.17	0.075
12	2.91	0.0008	-0.64	0.36	0.082
Average	4.07	0.0015	-5.26	0.37	0.026

Table 2.5. Monthly increments of climate parameters for Duluth, MN from scenario CGCM 3.1. All increments are additive, with indicated units.

Month	Ta (°C)	RH	Solar (W/m²)	Wind (m/s)	P (cm)
1	6.89	0.0006	-2.76	0.42	0.023
2	5.07	0.0005	-4.61	0.25	0.034
3	3.90	0.0004	0.89	0.10	0.013
4	4.31	0.0011	-9.09	0.42	0.087
5	4.12	0.0017	-14.24	0.31	0.064
6	4.59	0.0023	4.66	0.77	0.032
7	3.80	0.0022	6.99	0.24	0.002
8	3.30	0.0018	3.69	0.20	0.026
9	3.49	0.0016	5.18	0.46	-0.020
10	3.19	0.0012	1.91	0.30	0.049
11	2.89	0.0007	-0.88	0.28	0.033
12	4.14	0.0005	-2.36	0.37	0.059
Average	4.14	0.0012	-0.88	0.34	0.033

2.6 Simulated Scenarios

To project climate change impact on coldwater stream temperatures the calibrated stream temperature models for Miller Creek, Chester Creek and South Branch discussed in Section 2.4 were each run for 7 cases summarized in Table 2.6. the cases are combinations of climate scenarios. The stream temperature model was run using either baseline (observed) climate data for the years 1961-2005 or incremented climate data to calculate surface heat transfer. The climate record length used for this study was limited by the availability of solar radiation data. Source water temperatures were either baseline temperatures or incremented temperatures, as described in Section 2.3 and 2.5. In this way, the effects of incremented surface heat transfer and incremented source water temperatures were analyzed both separately and combined.

Simulations for Miller Creek and Chester Creek were run using climate data from Duluth International Airport, while simulations for the South Branch of the Vermillion River were run using climate data from the Minneapolis/St. Paul International Airport. In all cases, simulations were made for 45 years (1961-2005) of climate data, using either the baseline or incremented data.

Table 2.6. Summary of stream temperature analysis cases. Surface heat transfer and source water temperatures were determined for either baseline climate or incremented climate.

Case	Surface Heat Transfer	Source Water Temperature	Average Stream Temperature Increase (ºC)		
			Miller Creek	Chester Creek	South Branch
1	Baseline	Baseline	-	-	-
2	CGCM 2.0	Baseline	1.5	1.3	1.8
3	Baseline	CGCM 2.0	2.5	2.8	2.7
4	CGCM 2.0	CGCM 2.0	4.1	4.1	4.6
5	CGCM 3.1	Baseline	1.4	1.2	1.5
6	Baseline	CGCM 3.1	2.1	2.3	2.2
7	CGCM 3.1	CGCM 3.1	3.4	3.5	3.6

Stream discharge was estimated for each case based on precipitation data, using relationships between discharge and precipitation developed for each stream. An example of the stream discharge vs. precipitation relationship is given in Figure 2.9 for Miller Creek. The RMSE (root-mean-square error) between the discharge vs. precipitation relationships in Figure 2.9 and actual discharges is 0.3 m^3/s. This significant error resulted in relative little error in simulated temperatures because the results were much more sensitive to stream morphometry, especially stream width and climate parameters, than to streamflow. For 2008 data, daily stream temperatures simulated using 1) observed discharge data and 2) estimated discharges using the relationship given in Figure 2.9 differed only by 0.3 ºC (root-mean-square difference). The groundwater inflow rates calibrated for 2008 (Table 2.1) were used for all analyses, because no good basis was found to predict e.g. monthly variations of groundwater inflow rates.

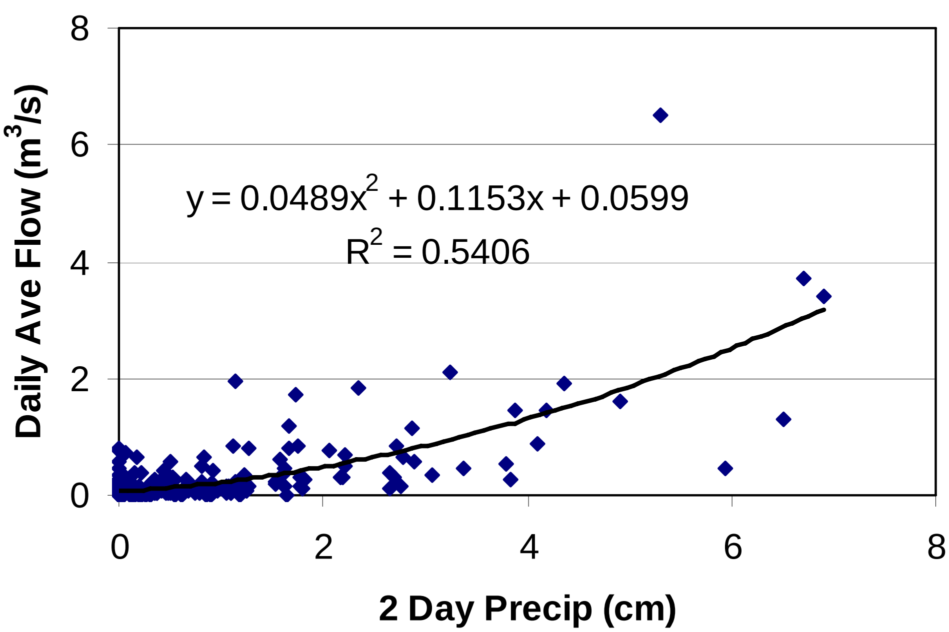

Figure 2.9. Daily average streamflow vs. 2-day antecedent total precipitation for Miller Creek, 1997-1998 and 2007-2008.

2.7 Simulation Results

The simulated stream temperature increases, averaged over all days, months (May to September) and years (1961-2005) of the entire simulation period are given for each of the seven simulated cases (scenarios) and each stream in Table 2.6. Overall, the three study streams showed similar temperature increases. The full CGCM 2.0 scenario (case 4) gave an average increase in stream temperature from 4.1 to 4.6ºC, whereas the full CGCM 3.1 scenario (case 7) gave only from 3.4 to 3.6ºC for the three streams. This is not surprising given that the average air temperature increase (Duluth and Minneapolis/St/Paul) was 4.1C for CGCM2.0 and 5.0 for CGCM 3.1 (Tables 2.3, 2.4 and 2.5).

Increases in direct atmospheric heat transfer to the stream as well as increases in source water temperatures figure prominently in the overall stream temperature response. Source water temperature changes give the larger response in stream temperature for all three study streams and both climate scenarios. South Branch had slightly higher total stream temperature increases compared to the Duluth streams (Miller Creek and Chester Creek), mainly because of lower effective riparian shading (Table 2.1). For the CGCM 3.1 scenario, the lower shading of South Branch was somewhat offset by the lower air temperature increments for Minneapolis compared to Duluth, with the result that the three study streams had very similar temperature increases.

Detailed information on monthly stream temperature simulation results is given in Tables 2.7 to 2.12 for each of the three study streams and the two climate change scenarios. The seasonal variation of stream temperatures and of temperature increases has been plotted in Figures 2.10 to 2.13. For each study stream and climate scenario, the stream temperature increase varied from month to month, driven by corresponding increments in climate parameters. The standard deviations of the daily stream temperature increments are quite small (< 0.5ºC) in all cases. This suggests that the coldwater stream temperature increases due to climate change are relatively uniform, independent of the daily variations in flow and baseline climate conditions.

For the CGCM 3.1 climate scenario, the highest stream temperature increase occurred in June for Miller Creek and Chester Creek and in July/August for South Branch. Overall, the stream temperature increments were slightly lower than the air temperature increments. The exception is the response of South Creek to climate scenario CGCM 3.1; South Creek's stream temperature increases due to the combined effects of surface heat transfer and source water temperature increases were up to 0.5ºC higher than the associated air temperature increments (Figure 2.13). For the CGCM 2.0 scenario, temperature increments for all three study streams were slightly higher than the air temperature increment in July. While atmospheric heat transfer causes stream temperature to track air temperature at the daily time scale, the less variable seasonal distribution of the source water temperature increments tends to give more uniform stream temperature increases.

The ratio of the average stream temperature increment to the average air temperature increment given in this section is 0.9 for Miller Creek and Chester Creek for both climate scenarios. This is substantially higher than the slope of the observed daily stream temperature vs. daily air temperature slopes given in Table 2.2 (0.60 for Miller Creek, 0.43 for Chester Creek). For South

Branch, the average stream temperature – air temperature increment ratio is 1.0 for CGCM 2.0 and 1.1 for CGCM 3.1, more than double the slope (0.43) of the observed stream temperature – air temperature plot. This suggests that observed, short term (daily) variations in stream temperature with air temperature are not representative of, and under-predict the long term response of stream temperatures to air temperature increases, mainly because of changes in source water temperature that do not appear at short times scales.

Table 2.7. Projected stream temperatures of Miller Creek in response to the CGCM 2.0 climate scenario. SD = standard deviation of daily values.

Mean Monthly Stream Temperatures (^oC)								
	Case 1 (Baseline)				Case 2			
Month	Mean	SD	Max	Min	Mean	SD	Max	Min
May	9.3	2.5	16.1	1.8	11.1	2.6	18.5	3.6
June	14.8	1.9	20.9	8.9	16.2	1.9	23.0	10.7
July	17.6	1.4	21.2	12.7	18.8	1.3	22.5	14.1
August	16.9	1.4	22.0	12.5	18.6	1.5	24.5	14.1
September	12.9	2.2	19.7	7.6	14.4	2.3	21.6	8.9
	Case 3				Case 4			
Month	Mean	SD	Max	Min	Mean	SD	Max	Min
May	12.0	2.5	18.7	4.3	13.8	2.6	20.8	6.1
June	17.3	1.9	23.0	11.5	18.8	1.9	25.1	13.3
July	20.1	1.3	23.3	14.9	21.4	1.3	24.8	16.5
August	19.3	1.4	24.1	15.0	21.2	1.5	26.5	16.8
September	15.4	2.1	21.9	9.9	16.9	2.2	23.8	11.4
Mean Monthly Stream Temperature Increments (^oC)								
	Case 2 - Case 1				Case 3 - Case 1			
Month	Mean	SD	Max	Min	Mean	SD	Max	Min
May	1.8	0.3	2.7	1.1	2.7	0.2	3.2	2.1
June	1.4	0.2	2.2	0.9	2.6	0.2	3.1	2.0
July	1.2	0.2	2.0	0.7	2.5	0.2	3.0	2.0
August	1.8	0.2	2.5	0.9	2.5	0.2	3.0	1.9
September	1.5	0.2	2.2	0.6	2.5	0.2	3.0	1.9
	Case 4 - Case 1							
Month	Mean	SD	Max	Min				
May	4.4	0.2	5.0	3.9				
June	4.1	0.1	4.8	3.6				
July	3.8	0.1	4.5	3.4				
August	4.3	0.1	4.6	3.7				
September	4.0	0.1	4.4	3.2				

Table 2.8. Projected stream temperatures of Miller Creek in response to the CGCM 3.1 climate scenario. SD = standard deviation of daily values.

Mean Monthly Stream Temperatures								
	Case 1 (Baseline)				Case 2			
Month	Mean	SD	Max	Min	Mean	SD	Max	Min
May	9.3	2.5	16.1	1.8	10.6	2.6	18.0	3.2
June	14.8	1.9	20.9	8.9	16.5	2.0	23.7	10.1
July	17.6	1.4	21.2	12.7	19.0	1.5	23.0	14.0
August	16.9	1.4	22.0	12.5	18.1	1.5	23.9	13.5
September	12.9	2.2	19.7	7.6	14.1	2.3	21.5	8.5
	Case 3				Case 4			
Month	Mean	SD	Max	Min	Mean	SD	Max	Min
May	11.5	2.5	18.3	3.8	12.8	2.6	20.1	5.2
June	17.0	1.9	22.7	11.1	18.5	2.0	25.3	12.2
July	19.8	1.3	23.0	14.6	21.2	1.4	24.9	16.0
August	19.0	1.4	23.8	14.5	20.1	1.5	25.6	15.6
September	14.9	2.2	21.5	9.3	16.0	2.3	23.3	10.2

Mean Monthly Stream Temperature Increments								
	Case 2 - Case 1				Case 3 - Case 1			
Month	Mean	SD	Max	Min	Mean	SD	Max	Min
May	1.3	0.2	2.0	0.8	2.2	0.1	2.6	1.7
June	1.7	0.3	2.7	1.0	2.2	0.2	2.6	1.7
July	1.4	0.2	2.1	0.9	2.2	0.2	2.6	1.7
August	1.2	0.2	1.9	0.8	2.1	0.2	2.6	1.6
September	1.2	0.2	1.9	0.7	2.0	0.1	2.4	1.5
	Case 4 - Case 1							
Month	Mean	SD	Max	Min				
May	3.5	0.1	4.2	3.2				
June	3.8	0.2	4.4	3.3				
July	3.6	0.1	3.9	3.2				
August	3.3	0.1	3.6	3.0				
September	3.1	0.2	3.6	2.7				

Table 2.9. Projected stream temperatures of Chester Creek in response to the CGCM 2.0 climate scenario. SD = standard deviation of daily values.

Mean Monthly Stream Temperatures

	Case 1 (Baseline)				Case 2			
Month	Mean	SD	Max	Min	Mean	SD	Max	Min
May	8.9	2.4	15.1	2.0	10.4	2.5	17.2	3.6
June	14.3	1.7	19.9	9.1	15.5	1.7	21.7	10.6
July	17.1	1.2	20.4	12.9	18.1	1.2	21.4	14.1
August	16.5	1.2	21.1	12.7	18.0	1.3	23.1	14.1
September	12.8	2.0	18.8	7.9	14.0	2.1	20.4	9.1

	Case 3				Case 4			
Month	Mean	SD	Max	Min	Mean	SD	Max	Min
May	11.8	2.4	17.9	4.8	13.3	2.4	19.8	6.3
June	17.2	1.7	22.3	11.9	18.4	1.7	24.1	13.4
July	19.9	1.1	22.7	15.3	21.0	1.1	24.0	16.8
August	19.2	1.2	23.5	15.4	20.8	1.3	25.5	17.0
September	15.5	2.0	21.3	10.5	16.7	2.0	22.9	11.8

Mean Monthly Stream Temperature Increments

	Case 2 - Case 1				Case 3 - Case 1			
Month	Mean	SD	Max	Min	Mean	SD	Max	Min
May	1.5	0.2	2.4	0.9	2.9	0.2	3.4	2.4
June	1.2	0.2	1.9	0.7	2.8	0.2	3.3	2.3
July	1.0	0.1	1.7	0.6	2.8	0.2	3.2	2.3
August	1.5	0.2	2.1	0.8	2.7	0.2	3.2	2.2
September	1.2	0.2	1.8	0.5	2.7	0.2	3.2	2.1

	Case 4 - Case 1			
Month	Mean	SD	Max	Min
May	4.4	0.1	4.9	4.0
June	4.1	0.1	4.6	3.6
July	3.8	0.1	4.4	3.5
August	4.3	0.1	4.5	3.7
September	4.0	0.1	4.4	3.3

Table 2.10. Projected stream temperatures of Chester Creek in response to the CGCM 3.1 climate scenario. SD = standard deviation of daily values.

Mean Monthly Stream Temperatures

	Case 1 (Baseline)				Case 2			
Month	Mean	SD	Max	Min	Mean	SD	Max	Min
May	8.9	2.4	15.1	2.0	10.0	2.5	16.7	3.2
June	14.3	1.7	19.9	9.1	15.8	1.8	22.4	10.1
July	17.1	1.2	20.4	12.9	18.4	1.3	21.9	14.0
August	16.5	1.2	21.1	12.7	17.5	1.3	22.7	13.6
September	12.8	2.0	18.8	7.9	13.8	2.1	20.3	8.8
	Case 3				Case 4			
Month	Mean	SD	Max	Min	Mean	SD	Max	Min
May	11.3	2.4	17.5	4.3	12.4	2.5	19.1	5.4
June	16.8	1.7	22.0	11.5	18.1	1.8	24.3	12.5
July	19.5	1.1	22.4	15.0	20.7	1.2	24.1	16.3
August	18.8	1.2	23.2	14.9	19.8	1.3	24.7	15.8
September	14.9	2.0	20.9	9.9	15.9	2.1	22.3	10.7

Mean Monthly Stream Temperature Increments

	Case 2 - Case 1				Case 3 - Case 1			
Month	Mean	SD	Max	Min	Mean	SD	Max	Min
May	1.1	0.2	1.8	0.7	2.4	0.1	2.8	2.0
June	1.5	0.2	2.5	0.9	2.4	0.1	2.8	1.9
July	1.2	0.2	1.8	0.8	2.4	0.1	2.8	1.9
August	1.0	0.1	1.7	0.6	2.3	0.1	2.8	1.8
September	1.0	0.2	1.7	0.5	2.1	0.1	2.5	1.7
	Case 4 - Case 1							
Month	Mean	SD	Max	Min				
May	3.5	0.1	4.2	3.2				
June	3.8	0.2	4.4	3.4				
July	3.6	0.1	4.0	3.3				
August	3.3	0.1	3.7	3.1				
September	3.1	0.1	3.7	2.7				

Table 2.11. Projected stream temperatures of South Branch in response to the CGCM 2.0 climate scenario. SD = standard deviation of daily values.

Mean Monthly Stream Temperatures

	Case 1 (Baseline)				Case 2			
Month	Mean	SD	Max	Min	Mean	SD	Max	Min
May	12.8	2.2	19.4	6.2	15.0	2.4	23.0	8.0
June	15.9	2.0	22.0	9.4	17.6	2.1	24.3	11.5
July	17.5	1.7	23.5	12.0	18.8	1.7	25.0	13.3
August	16.9	1.7	21.9	12.3	19.0	1.8	24.6	14.3
September	14.3	2.2	20.2	8.3	16.1	2.3	22.7	10.3
	Case 3				Case 4			
Month	Mean	SD	Max	Min	Mean	SD	Max	Min
May	15.5	2.2	21.6	8.7	17.7	2.4	24.8	10.7
June	18.5	1.9	24.0	11.7	20.4	2.0	26.7	13.9
July	20.2	1.6	25.5	15.0	21.6	1.6	27.2	16.5
August	19.6	1.6	24.2	14.8	21.8	1.7	26.9	17.2
September	17.1	2.1	22.6	10.6	18.8	2.2	24.8	12.7

Mean Monthly Stream Temperature Increments

	Case 2 - Case 1				Case 3 - Case 1			
Month	Mean	SD	Max	Min	Mean	SD	Max	Min
May	2.3	0.4	3.8	1.2	2.7	0.3	3.7	1.8
June	1.8	0.3	3.1	1.0	2.7	0.3	3.6	1.7
July	1.3	0.2	2.6	0.8	2.7	0.3	3.6	1.5
August	2.1	0.3	2.8	1.1	2.7	0.3	3.8	1.8
September	1.7	0.3	2.6	0.7	2.8	0.3	3.7	1.8
	Case 4 - Case 1							
Month	Mean	SD	Max	Min				
May	4.9	0.3	6.0	4.3				
June	4.5	0.2	5.5	3.8				
July	4.1	0.2	5.0	3.5				
August	4.9	0.1	5.2	3.9				
September	4.5	0.1	5.0	3.5				

Table 2.12. Projected stream temperatures of South Branch in response to the CGCM 3.1 climate scenario. SD = standard deviation of daily values.

Mean Monthly Stream Temperatures								
	Case 1 (Baseline)				Case 2			
Month	Mean	SD	Max	Min	Mean	SD	Max	Min
May	12.8	2.2	19.4	6.2	14.1	2.4	21.6	7.1
June	15.9	2.0	22.0	9.4	17.4	2.1	24.1	11.0
July	17.5	1.7	23.5	12.0	19.2	1.8	25.5	13.2
August	16.9	1.7	21.9	12.3	18.5	1.8	24.2	13.6
September	14.3	2.2	20.2	8.3	15.8	2.4	22.4	9.7
	Case 3				Case 4			
Month	Mean	SD	Max	Min	Mean	SD	Max	Min
May	14.9	2.2	21.2	8.2	16.2	2.4	23.1	9.2
June	18.0	1.9	23.6	11.3	19.5	2.1	25.8	12.8
July	19.7	1.6	25.1	14.5	21.2	1.7	27.1	15.6
August	19.1	1.6	23.8	14.3	20.6	1.7	25.8	15.7
September	16.5	2.1	22.1	10.1	17.9	2.3	24.1	11.6

Mean Monthly Stream Temperature Increments								
	Case 2 - Case 1				Case 3 - Case 1			
Month	Mean	SD	Max	Min	Mean	SD	Max	Min
May	1.4	0.3	2.4	0.6	2.2	0.2	3.0	1.5
June	1.6	0.2	2.5	0.9	2.1	0.2	2.8	1.3
July	1.6	0.2	2.5	1.1	2.1	0.2	2.9	1.2
August	1.6	0.2	2.3	0.9	2.2	0.2	3.1	1.5
September	1.5	0.2	2.2	0.8	2.2	0.2	3.0	1.5
	Case 4 - Case 1							
Month	Mean	SD	Max	Min				
May	3.4	0.2	4.1	3.0				
June	3.6	0.2	4.1	3.1				
July	3.7	0.1	4.1	3.4				
August	3.7	0.1	4.1	3.3				
September	3.6	0.1	4.0	3.2				

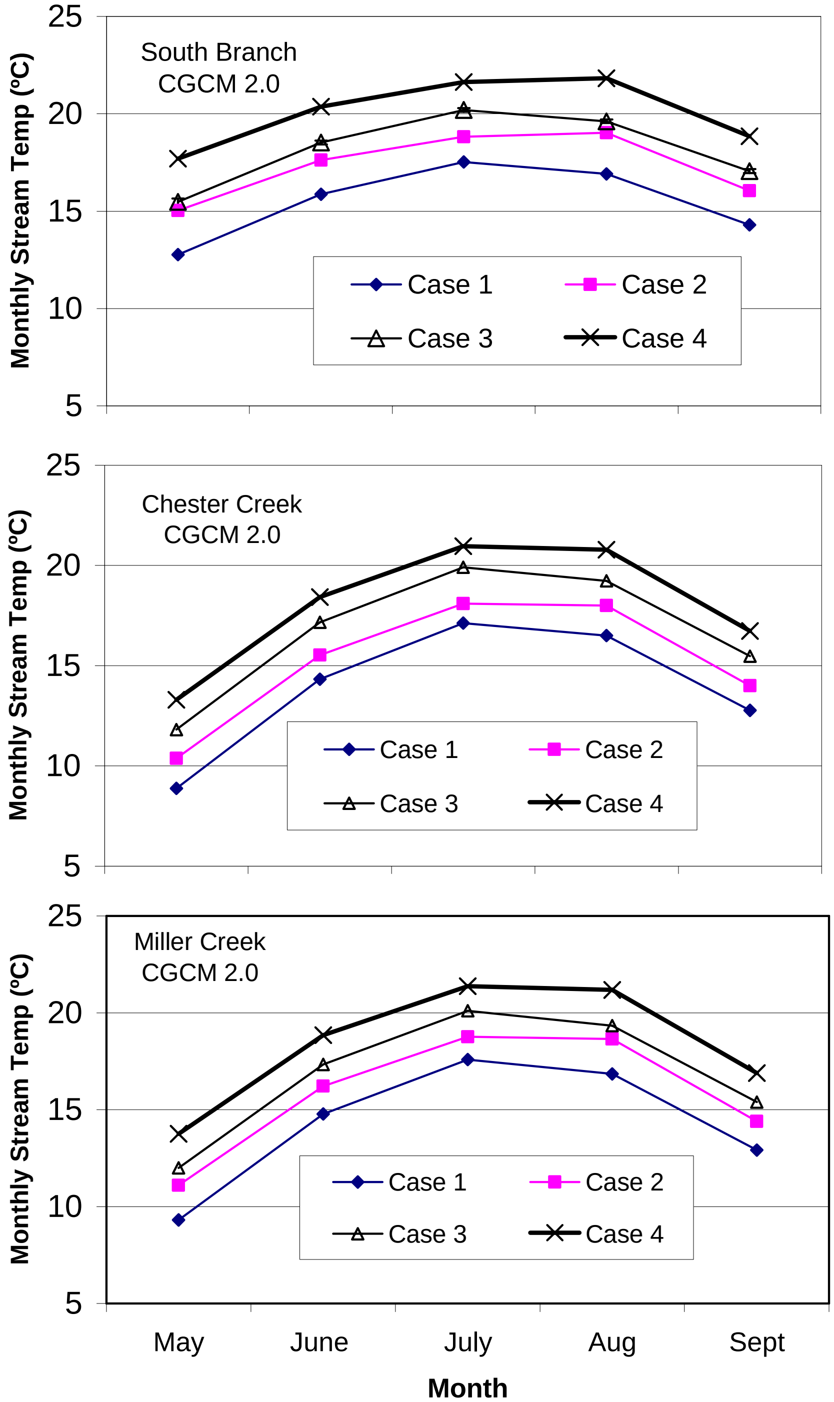

Figure 2.10. Mean monthly stream temperatures for the CGCM 2.0 scenario (Cases 2, 3, 4) and baseline (Case 1) for South Branch, Chester Creek, and Miller Creek.

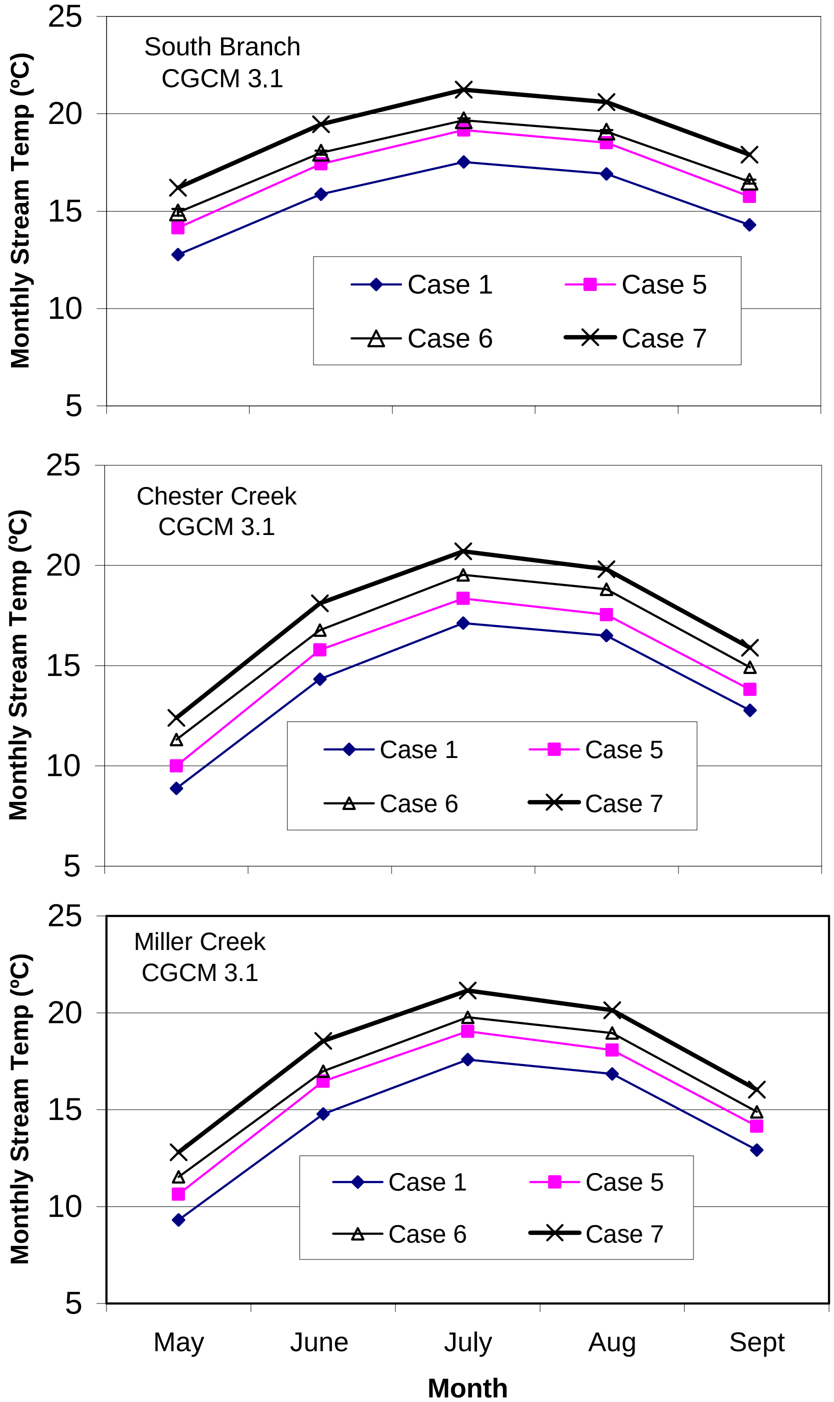

Figure 2.11. Mean monthly stream temperatures for the CGCM 3.1 scenario (Cases 5, 6, 7) and baseline (Case 1) for South Branch, Chester Creek, and Miller Creek.

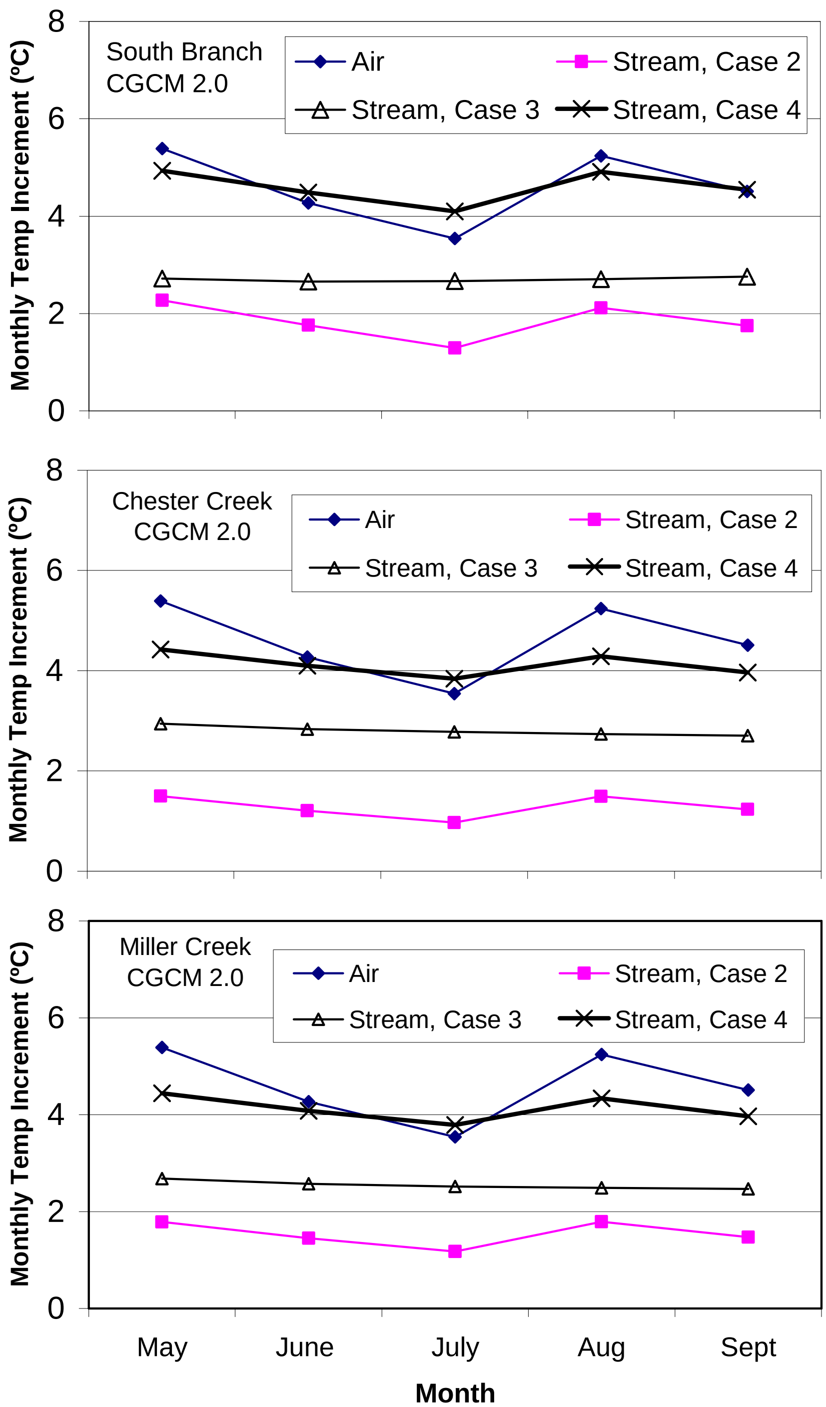

Figure 2.12. Mean monthly air and stream temperature increments for the CGCM 2.0 scenario (Cases 5, 6, 7) for South Branch, Chester Creek, and Miller Creek.

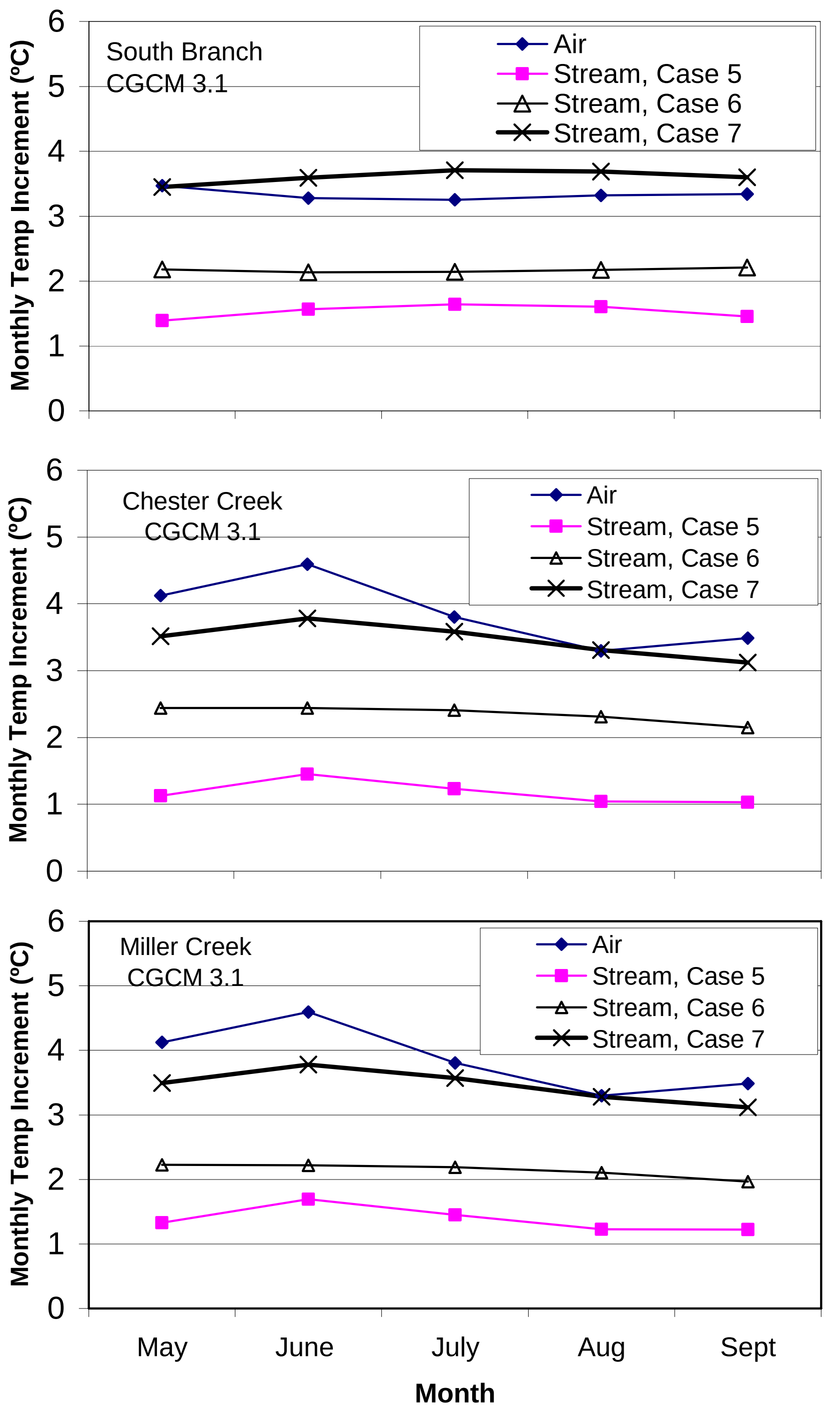

Figure 2.13. Mean monthly air and stream temperature increments for the CGCM 3.1 scenario (Cases 5, 6, 7) for South Branch, Chester Creek, and Miller Creek.

2.8 Summary and Conclusions, Part II

Coldwater streams in Minnesota provide habitat to valuable trout populations, and climate change poses a threat to this habitat. A study of three coldwater streams, which are designated trout streams in Minnesota, has therefore been conducted to assess the potential magnitude of stream temperature changes in these streams. Two of these study streams, Miller Creek and Chester Creek, are located in Duluth and one, the South Branch of the Vermillion River is located south of the Twin Cities. Deterministic stream temperature models were used to characterize the response of the water temperatures in the three streams to projected climate change scenarios. The models include both the heat transfer between the streams and the atmosphere and the potential warming of the cold water sources. These coldwater sources are groundwater in the Vermillion River basin for the South Branch, and wetlands for the two North Shore streams.

Overall, water temperatures in the streams were projected to increase between 4 and 5°C for the CGCM 2.0 (doubling of atmospheric CO2) climate change scenario, and between 3 and 4°C for the CGCM 3.1 A1B (rapid economic growth) climate change scenario. Estimated increases in source water temperatures accounted for approximately 60% of the total stream temperature increase due to climate change; increases in atmospheric heat transfer provided approximately 40%. The source water temperature in the (shallow) groundwater aquifer was assumed to increase the same as the mean annual air temperature (4 to 5°C) over a period of many years because mean annual ground temperatures are known to be similar to mean annual air temperatures above the ground (Taylor and Stefan 2009); the increase in wetland temperature was predicted by a wetland temperature model (Herb et al. 2007).to be 3 to 4°C, i.e. less than the groundwater temperature increase because of evaporative cooling.

The ratio of the stream temperature increment to air temperature increment was found to vary from 0.8 to 1.08, much larger than the slope of the observed daily stream temperature versus daily air temperature relationship. For the CGCM 2.0 CO2 scenario (doubling of atmospheric CO2), stream temperature increments projected by this study are 4 to 5°C. These increments are larger than those projected by previous climate change studies based on air temperature – stream temperature regression analysis (2 to 3°C) (Mohseni et al. 1999, Morrill et al. 2005).

It has been demonstrated that a deterministic stream temperature model based on the equilibrium temperature concept can reveal the response of coldwater stream temperatures to climate change at local scales. To project stream temperatures, the model requires climate data, stream width, source water (e.g. groundwater) input rates and temperatures. It is necessary to characterize the response of source water quantities and temperatures to climate change for each hydrogeologic setting.

It has also been demonstrated in this study that source water temperatures figure prominently in the response of stream temperatures to long term climate change. Although the field measurements and model calibration procedures give some evidence that the seasonal source water temperatures used in this study are appropriate, further work is needed on both groundwater and wetland systems to better characterize both the hydrology and heat transfer processes that control these systems.

Karst systems, e.g. in the driftless area of southeastern Minnesota and southwestern Wisconsin, may act quite differently from the shallow sand aquifer (Vermillion River) or wetland systems (Duluth streams) considered in this study . Possible changes in available source water quantities and input rates in addition to source water temperatures should also be investigated, as changes in precipitation patterns and evapotranspiration are expected to accompany long term climate change.

Winter conditions were not considered in this study. Long term changes in groundwater temperatures and air temperatures may markedly affect winter water temperatures and ice cover conditions, and therefore impact winter habitat for fish and invertebrates.

Acknowledgments

Funding for this study was provided by the Environmental and Natural Resources Trust Fund as recommended by the Legislative-Citizens Commission on Minnesota Resources (LCCMR), St. Paul, MN. The grant was coordinated by Lucinda Johnson from the Natural Resources Research Institute in Duluth. Stream flow and temperature data for the Vermillion River were supplied by Travis Bistodeau of the Dakota County Soil and Water Conservation District and by the U.S. Geological Survey. Stream flow and temperature data for the Duluth streams were supplied by the South St. Louis Soil and Water Conservation District and Duluthstreams.org. Streambed temperature data were supplied by Dr. Kim Chapman of the Applied Ecological Services Inc. in St. Paul, MN. Canadian Centre for Climate Modeling and Analysis scenarios were obtained through Prof. Xing Fang, Auburn University. The authors thank these individuals and organizations for their help and cooperation.

References

Bogan, T., Mohseni, O., and H.G. Stefan (2003), The stream temperature/equilibrium temperature relationship. *Water Resources Research* 39(9):1245-1256.

Bogan, T.R., H.G. Stefan and O. Mohseni (2004), Imprints of secondary heat sources on the stream temperature/equilibrium temperature relationship. *Water Resources Research* 40(12), W12510.

Brown, LE and D.M. Hannah (2007), Alpine stream temperature response to storm events. *Journal of Hydrometeorology* 8: 952-967.

Burkholder, B.K., Grant, G.E., Haggerty, R., Khangaonkar, T., and P.J. Wampler (2008). Influence of hyporheic flow and geomorphology on temperature of a large, gravel-bed river, Clackamas River, Oregon, USA. *Hydrologic Processes* 22: 941-953.

Caissie, D., (2006), The thermal regime of rivers: a review. *Freshwater Biology* 51:1389–1406.

Clark, M.E., Rose, A., Levine, D.A. and W.W. Hargrove (2001). Predicting climate change effects on Appalachian trout: combining GIS and individual-based modeling. *Ecological Applications* 11(1):161–178.

Detenbeck, N.E., Elonen, C.M., Taylor D.L., Anderson, L.E., Jicha, T.M., Batterman, S.L. 2003. Effects of hydrogeomorphic region, catchment storage and mature forest on baseflow and snowmelt stream water quality in second-order Lake Superior Basin tributaries. *Freshwater Biology* 48: 912-927.

Durance, I. and S.J. Ormerod (2007). Climate change effects on upland stream macroinvertebrates over a 25-year period. *Global Change Biology* 13: 942–957.

Eaton, J.G. , McCormick, J.H., Goodno, B.E., O'Brien D.G., Stefan H.G., Hondzo, M. and R.M. Scheller (1995). A field information-based system for estimating fish temperature tolerances. *Fisheries* 20(4):10-18.

Eckert, E.R.G., Drake, R.M. Jr. 1972. *Analysis of Heat and Mass Transfer.* McGraw-Hill, New York.

Edinger, J.E., D.W. Duttweiler and J.C. Geyer (1968), The response of water temperature to meteorological conditions, *Water Resources Research* 4(5): 1137-1145.

Edinger, J.E., D.K. Brady and J.C. Geyer (1974). Heat exchange and transport in the environment. *Report No. 14*, Electric Power Research Institute, Cooling Water Discharge Research Project (RP-49), Palo Alto, CA.

Emmons and Olivier Resources, Inc.(EOR). 2007. Vermillion River Headwaters groundwater recharge area inventory and protection plan. EOR Report. Oakdale, MN.

Erickson, T. and H.G. Stefan (2000). Linear air/water temperature correlations in streams during open water periods. *Journal of Hydrologic Engineering* 5(3): 317-321.

Erickson, T.O and Stefan, H.G. (2009). Natural groundwater recharge response to urbanization: Vermillion River watershed, Minnesota. *Journal of Water Resources Planning and Management* 135(6): 512-520.

Ficke AD, Myrick CA, Hansen LJ. (2007). Potential impacts of global climate change on freshwater fisheries. *Reviews in Fish Biology and Fisheries* 17:581–613.

Fitzpatrick, F.A., Peppler, M.C., DePhilip, M.M., Lee KE. (2006). Geomorphic characteristics and classification of Duluth-area streams, Minnesota. USGS Scientific Investigations Report 2006–5029, U.S. Department of the Interior, 54 pp.

Hari, R.E., Livingstone, D.M., Siber, R., Burkhardt-Holm, P., and H. Guttinger (2006). Consequences of climatic change for water temperature and brown trout populations in Alpine rivers and streams. *Global Change Biology* 12(1):10–26.

Herb W.R., Mohseni O., Stefan H.G. (2007). A model for mitigation of surface runoff temperatures by a wetland basin and a wetland complex. *Project Report No. 499*, St. Anthony Falls Laboratory, University of Minnesota. (available at http://home.safl.umn.edu/bmackay/pub/pr/pr499.pdf)

Herb, W.R. and H.G. Stefan (2008a). A flow and temperature model for the Vermillion River, Part I: Model development and baseflow conditions. *Project Report No. 517*, St. Anthony Falls Laboratory, University of Minnesota. (available at http://home.safl.umn.edu/bmackay/pub/pr/pr517.pdf)

Herb, W.R. and H.G. Stefan (2008b). A flow and temperature model for the Vermillion River, Part II: Response to surface runoff inputs, *Project Report No. 525*, St. Anthony Falls Laboratory, University of Minnesota. (available at http://home.safl.umn.edu/bmackay/pub/pr/pr525.pdf)

Janke, B., Herb, W.R., Mohseni, O., and H.G. Stefan (2008). Estimation of groundwater input to the Vermillion River from observations of stream flow and stream temperature. *Project Report No. 523*, St. Anthony Falls Laboratory, University of Minnesota. (available at http://home.safl.umn.edu/bmackay/pub/pr/pr523.pdf)

Johnson, S.L. (2004). Factors influencing stream temperatures in small streams: substrate effects and a shading experiment. *Canadian Journal of Fisheries and Aquatic Sciences* 61: 913–923.

Kim, K.S., and S.C. Chapra (1997). Temperature model for highly transient shallow streams, *Journal of Hydraulic Engineering* 123(1):30–40.

Meisner, J.D., Rosenfeld, J.S., Regier, H.A. (1988). The role of groundwater in the impact of climate warming on stream salmonids. *Fisheries* 13:2-8.

Mohseni, O. and H. G. Stefan (1998). A non-linear regression model for weekly stream temperatures. *Water Resources Research* 34(10): 2685-2692.

Mohseni, O. and H. G. Stefan (1999). Stream temperature/air temperature relationship: a physical interpretation. *Journal of Hydrol*ogy 218:128-141.

Mohseni, O., Erickson, T.R., and H.G. Stefan (1999). Sensitivity of stream temperatures in the U.S. to air temperatures projected under a global warming scenario, *Water Resources Research* 35(12):3723-3733.

Morrill, J.C., Bales, R.C., Conklin, M.H. (2005). Estimating stream temperature from air temperature: Implications for future water quality. *Journal of Environmental Engineering* 131(1):139-146.

Nelson, K.C. and M.A. Palmer (2007). Stream temperature surges under urbanization and climate change: Data, models, and responses, *Journal of the American Water Resources Association.* 43(2): 440-452.

Ryan, P. J. and D.R.F. Harleman (1973). An analytical and experimental study of transient cooling pond behavior. Parsons Laboratory for Water Resources and Hydrodynamics Report No. 161, Massachusetts Institute of Technology, Cambridge, MA.

Sinokrot, B.A. and H.G. Stefan (1993). Stream temperature dynamics: measurements and modeling, *Water Resources Research* 29(7): 2299-2312.

Sinokrot, B.A. and H.G. Stefan (1994). Stream water temperature sensitivity to weather parameters, *Journal of Hydraulic Engineering,* 120(6): 722-736.

Stefan, H.G., Gulliver, J., Hahn, M., and A. Fu (1980). Analysis and Modeling of Water Temperature Dynamics in the USEPA Monticello Field Channels, Project Report No.193, St. Anthony Falls Hydraulic Laboratory, University of Minnesota, Minneapolis, MN, Parts I and II, 168 pp. (available at http://home.safl.umn.edu/bmackay/pub/pr/pr193.pdf)

Stefan H.G., Preud'homme, E.B. (1993). Stream temperature estimation from air temperature. *Water Resources Bulletin* 29: 27-45.

Story, A., Moore, R.D., and J.S. Macdonald (2003). Stream temperature in two shaded reaches below cutblocks and logging roads: downstream cooling linked to subsurface hydrology. *Canadian Journal of Forest Resources* 33, 1383-1396.

Tang, H.S., and T. R. Keen (2009). Analytical Solutions for Open-Channel Temperature Response to Unsteady Thermal Discharge and Boundary Heating, *Journal of Hydraulic Engineering* 135(4), 327-332.

Taylor, C. and Stefan, H.G. (2009). Shallow groundwater temperature response to climate change and urbanization. *Journal of Hydrology* 375: 601-612.

Theurer, F.D., Voos, K.A. and W.J. Miller (1984). Instream water temperature model. *Instream Flow Information Paper 16*, U.S. Fish and Wildlife Service, FWS/OBS-84/15.

US EPA (2005). One-dimensional riverine hydrodynamic and water quality model, U.S. Environmental Protection Agency, Athens, Georgia. (available at http://www.epa.gov/ATHENS/wwqtsc/html/epd-riv1.html)

Wang, L., J. Lyons and P. Kanehl (2003). Impacts of urban land cover on trout streams in Wisconsin and Minnesota. *Transactions American Fisheries Society* 132, 825–839.

Webb, B.W., Clack. P.D., and D.E. Walling (2003). Water-air temperature relationships in a Devon river system and the role of flow. *Hydrologic Processes* 17, 3069–3084.

Webb, B.W., Hannah, D.M., Moore, R.D., Brown, L.E. and F. Nobilis (2008). Recent advances in stream and river temperature research. *Hydrologic Processes* 22, 902-918.